The extension discrepancy and syn-rift subsidence deficit at rifted margins

Tim J. Reston

School of Geography, Earth and Environmental Sciences, University of Birmingham, Birmingham B15 2TT, UK (e-mail: t.j.reston@bham.ac.uk)

ABSTRACT: Across most rifted margins, the extension measured from fault geometries is far less than that required to explain whole crustal and lithospheric thinning. This 'extension discrepancy' is commonly explained through crustal depth-dependent stretching (DDS – perhaps better termed depth-dependent thinning, DDT). However, several independent lines of evidence (velocity structure, rheological modelling, reconstructions, ODP drilling results) show that the amount of DDT required to explain the extension discrepancy cannot have occurred. Instead, it is suggested that as extension increases, complex geometries arise which are not completely interpreted, leading to a massive underestimation of the amount of extension. The implications are that pre-rift and early syn-rift reservoir and source rocks are likely to be widely scattered across deep margins. In the absence of massive crustal DDT, the deficit in syn-rift subsidence observed at some margins can be explained by thermal and dynamic uplift, igneous addition or mantle serpentinization during rifting. But it is also possible that syn-rift subsidence has been systematically underestimated if local water level was substantially below global sea-level, as indicated at some margins by the formation of thick evaporites at the end of rifting.

KEYWORDS: *margin, rift, extension, subsidence*

INTRODUCTION

The McKenzie (1978) model provides a simple quantitative framework for predicting the subsidence of a basin or margin as a consequence of lithospheric extension. The model assumes constant volume and uniform extension throughout the lithosphere, relating various measurable quantities (the extension of the crust, the thinning of the crust, subsidence both during and after rifting and heat flow) to a single factor β, called the stretching factor (Fig. 1). The power of the model means that simply measuring one of these parameters allows the others to be deduced; measurement of two provides independent verification of the accuracy of the measurements (e.g. Wood & Barton 1983). However, it was suggested (Ziegler 1983) that the amount of extension that could be measured from the faults imaged on seismic data was insufficient to explain the amount of crustal thinning required to explain the subsidence. Various means were invoked to explain this 'extension discrepancy'

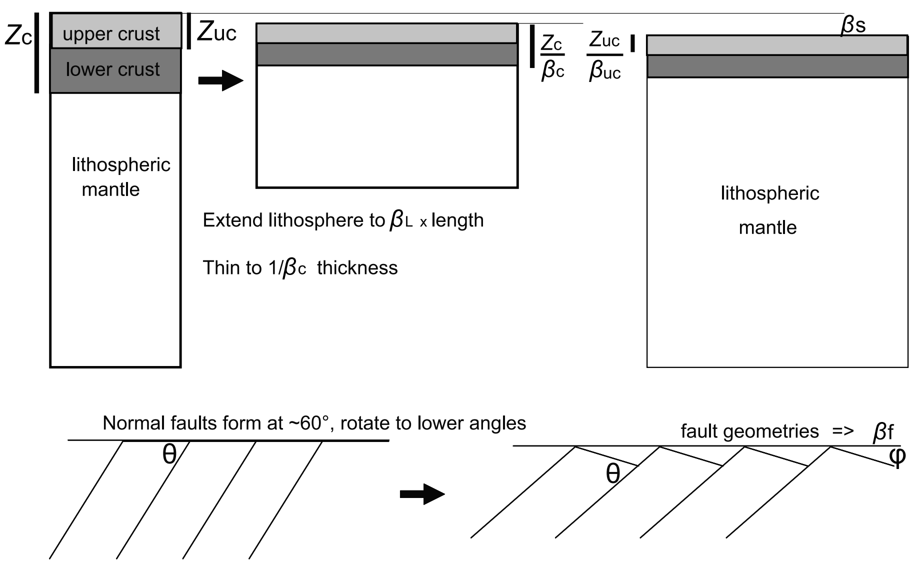

Fig. 1. McKenzie (1978) model for lithospheric extension. Stretching factors can be defined from changes in length (β_L), changes in crustal thickness (β_c), changes in thickness of the upper crust (β_{uc}), subsidence (β_s) and fault geometry (β_f). At rifted margins these do not always appear to agree.

Petroleum Geoscience, Vol. **15** 2009, pp. 217–237
DOI 10.1144/1354-079309-845

1354-0793/09/$15.00 © 2009 EAGE/Geological Society of London

(listric faulting – McKenzie 1978; inclined shear – White *et al.* 1986), which was finally resolved for most rift basins once imaging methods improved (White 1990; Kusznir & Karner 2007), and once it was realized that basins commonly had undergone multiple phases of rifting (e.g. Giltner 1987) and that up to 50% of the extension occurs through distributed deformation (Walsh *et al.* 1991; Marrett & Allmendinger 1992), sometimes referred to as sub-seismic faulting.

Like rift basins, rifted margins form through lithospheric extension, but, in this case, leading to the break-up of the continents. Typically, such margins show a crust affected by normal faulting and thinning toward zero as the continent–ocean transition is approached (Fig. 2), and have been explained or analysed by the McKenzie model almost since the model was developed (e.g. Le Pichon & Sibuet 1981). However, many authors have recently noted that the amount of crustal thinning that can be deduced from subsidence or from crustal thicknesses inferred from seismic data $(1 - 1/\beta_f)$ greatly exceeds that predicted $(1 - 1/\beta_f)$ by the measurable extension along the normal faults that cut across the upper crust (β_f) (Sibuet 1992; Driscoll & Karner 1998; Watcharanantakul & Morley 2000; Meredith & Egan 2002; Davis & Kusznir 2004; Kusznir & Karner 2007). Thus, the extension discrepancy (Fig. 3), which was originally noted for the North Sea (Ziegler 1983), has now been described for the following margins and deep basins: Pattani (Watcharanantakul & Morley 2000), Black Sea (Meredith & Egan 2002, but questioned by Shillington *et al.* 2008), Voring (Kusznir *et al.* 2005), Lofoten (Kusznir *et al.* 2005), Goban Spur (Davis & Kusznir 2004), Galicia Bank (Sibuet 1992; Davis & Kusznir 2004), the Galicia Interior Basin (Davis & Kusznir 2004), S China Sea (Clift *et al.* 2001; Davis & Kusznir 2004), Exmouth Plateau (Driscoll & Karner 1998) and the Lower Congo Basin (Contrucci *et al.* 2004*a*). The basic discrepancy is that the amount of extension observed from fault geometries (β_f) is less than that required to explain the crustal thinning and subsidence (β_f), i.e. $\beta_f \ll \beta_c$. A possibly related issue is that some margins appear to have subsided little during rifting but rapidly following the end of rifting, again in breach of the predictions of the McKenzie model. This, I will term the 'syn-rift subsidence deficit'.

Two end-member explanations for the extension discrepancy exist. First is the view that the fault geometries reveal all or nearly all of the extension of the brittle upper crust and that the extension discrepancy is due to the thinning of most of the crust by some other process. This depth-dependent thinning (DDT) is generally assumed to occur through depth-dependent stretching (DDS; Driscoll & Karner 1998; Watcharanantakul & Morley 2000; Meredith & Egan 2002; Clift *et al.* 2001; Davis & Kusznir 2004; Kusznir *et al.* 2005; Kusznir & Karner 2007), although other possibilities, such as delamination, should perhaps not be excluded. Depth-dependent stretching within the crust (crustal DDS) as an explanation for the extension discrepancy implies that $\beta_f \sim \beta_{uc} \ll \beta_c$. Indeed, several papers (e.g. Clift *et al.* 2001; Davis & Kusznir 2004; Kusznir & Karner 2007) assume this equivalence and, when plotting β_f, actually label it as β_{uc}. However, we shall see that this assumption may not be correct.

The second explanation for the extension discrepancy is that β_{uc} has been severely underestimated, as β_f does not record all the extension of the upper crust, as turned out to be the case for the North Sea and similar basins. Thus, the end-member possibility is that extension is fundamentally uniform with depth but not fully recognized in the upper crust, i.e. that $\beta_f \ll \beta_{uc} \sim \beta_c$.

One way that extension may go unrecognized is if it occurs through distributed deformation (Marrett & Allmendinger 1992), one of the ways that the extension discrepancy was resolved for the North Sea. However, although distributed deformation does undoubtedly occur at margins as well as in rift basins and, it is generally assumed, may accommodate up to 50% of the extension seismically measurable from fault heaves, this amount is insufficient to explain the extension discrepancy (Davis & Kusznir 2004; Reston 2007*a*). Alternatively, there may be other types of unrecognized faulting (Reston 2007*a*), discussed further below.

Of course it is also possible that the extension discrepancy is explained by a combination of both crustal DDS and unrecognized faulting, so that $\beta_f < \beta_{uc} < \beta_c$. However, it is useful first to investigate whether the two end-member solutions can explain the discrepancy and whether either can be largely ruled out.

DEPTH-DEPENDENT STRETCHING (DDS) AND THINNING (DDT)

The idea that the stretching of the lithosphere is not completely uniform (as assumed by McKenzie 1978) has been around for almost as long as the stretching model. Royden & Keen (1980), for instance, explored this possibility, as well as considering the effect of igneous addition during rifting (breaking the constant volume assumption of the McKenzie model). Hellinger & Sclater (1983) and Rowley & Sahagian (1986) both considered the effect of stretching the mantle lithosphere by a different amount to the crust and the idea was refined so that the total amount of extension of the lithosphere across the basin was constant, but with a different distribution at different lithospheric levels. The mechanism for such heterogeneous lithospheric extension might involve an outward-dipping zone of extension in the mantle (Rowley & Sahagian 1986), perhaps controlled by outward-dipping but symmetrically disposed shear zones (Reston 1993; Crosby *et al.* 2009), and/or a zone of strong shearing in the lower crust transferring deformation between the crust and mantle (Reston 1993) which have different but overlapping strain distributions. As lithospheric thinning is akin to necking, the lateral strain distribution at different lithospheric levels may also approximate a Gaussian distribution; DDS can thus be represented by different Gaussian functions at different lithospheric levels (e.g. White & McKenzie 1988).

Although the term depth-dependent stretching is used widely, it is fundamentally depth-dependent thinning that is important in discussions of subsidence, crustal structure and lithospheric structure. This is not just a matter of semantics but has practical implications for the description of DDS. For instance, simple symmetrical lithospheric DDS, in which the crust is always stretched twice as much at the rift axis as the underlying lithospheric mantle, does not on its own provide an explanation for the unroofing of continental mantle within the continent–ocean transition (COT) as, at high stretching factors, the thickness of both the crust and the lithospheric mantle converge towards zero. However, if the thinning factor (defined as $1 - 1\ \beta$) in the crust at the rift axis is always 50% greater than that of the mantle lithosphere, the latter will be unroofed when the mantle thinning factor has reached 0.67 (Fig. 4). Excess thinning of the crust at the rift axis has to be balanced by excess thinning of the mantle underneath the rift flanks, providing a simple explanation for their temporary uplift during rifting and the subsequent development of post-rift onlap (White & McKenzie 1988).

However, lithospheric DDS or DDT *per se* do not provide an explanation for the extension discrepancy as depth-dependent stretching and thinning within the *crust* is required if $\beta_f \sim \beta_{uc} \ll \beta_c$. Crustal DDS (or rather DDT) is a particularly

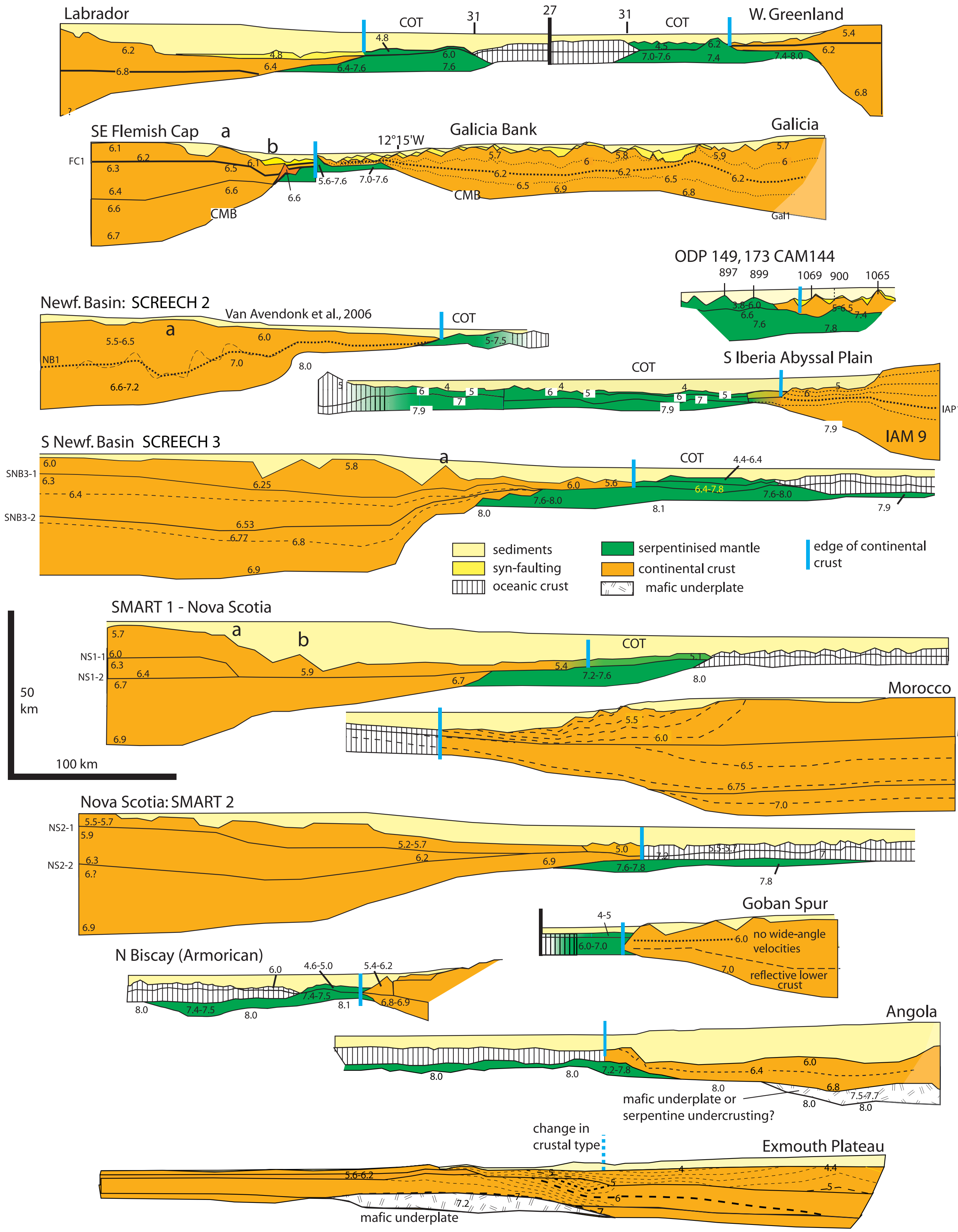

Fig. 2. Sections through magma-poor conjugate rifted margin pairs: Labrador–Greenland (Chian *et al.* 1995); SE Flemish Cap–Galicia (Funck *et al.* 2003; Zelt *et al.* 2003); Newfoundland Basin (van Avendonk *et al.* 2006) and S Newfoundland Basin (Lau *et al.* 2006)–Iberia Abyssal Plain (Dean *et al.* 2001); Nova Scotia (Funck *et al.* 2004)–Morocco (Contrucci *et al.* 2004*b*) and two non-conjugate margins: Goban Spur (Bullock & Minshull 2005), Armorican Margin (Thinon *et al.* 2003). All margins exhibit similar features (very thinned crust, little magmatism, mantle serpentinization, mantle unroofing) except for Morocco (no obvious serpentinization). For comparison, two other margins are also shown: Congo–Angola (Contrucci *et al.* 2004*a*) where underplating may have occurred under the continental slope, and Exmouth Plateau (Kusznir & Karner 2007), with probable underplating and no serpentinization. CMB, crust–mantle boundary; COT, continent–ocean transition.

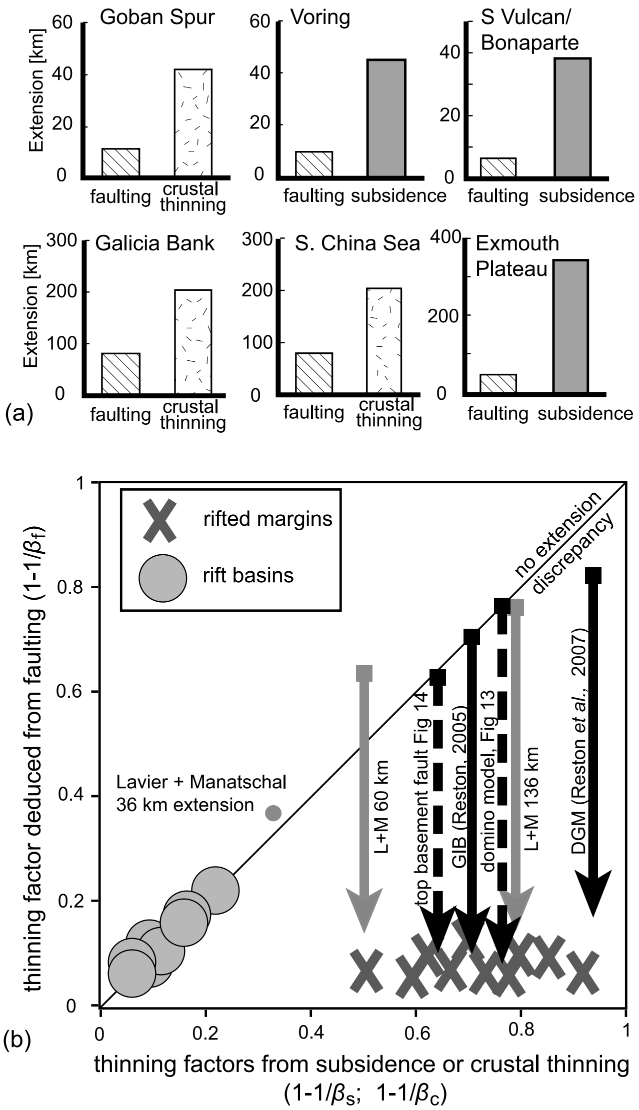

Fig. 3. (**a**) Estimates of extension from fault geometries or subsidence for six margins. Modified and relabelled after Davis & Kusznir (2004). (**b**) Cross-plot of thinning factor deduced from subsidence or crustal thinning against that determined from estimates of fault geometry, redrawn and relabelled from Kusznir & Karner (2007). Rift basins plot along the diagonal (no extension discrepancy), whereas rifted margins consistently plot in the bottom right corner, indicating that there is far too little measurable faulting to explain crustal thinning and subsidence. Also shown are the estimates of these thinning factor derived from simple polyphase faulting (Fig. 13), from top basement faulting (Fig. 14) as broken arrows, from numerical model (Fig. 9) of Lavier and Manatschal (2006 – grey arrows), and observations/restorations of the Galicia Interior Basin (GIB) and Deep Galicia Margin (DGM) (black arrows). In all cases, the tail of the arrow indicates fully measured extension, point of the arrow indicates likely underestimate of extension.

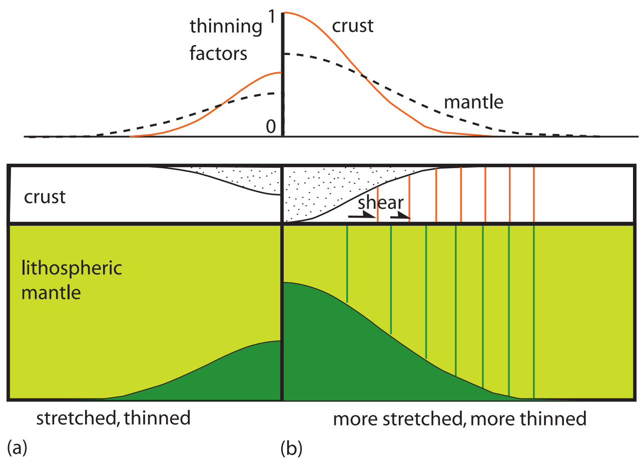

Fig. 4. (**a**) Lithospheric depth-dependent thinning model required to explain post-rift onlap, modified after White & McKenzie (1988). (**b**) Same model in which thinning factors are doubled at the basin axis but unaltered at the basin flanks (stretching factors adjusted accordingly): lithospheric mantle is exhumed at the rift axis where the crust has thinned to zero. Post-rift onlap and mantle unroofing may be manifestations of the same style of lithospheric DDT at different amounts of thinning. Note also significant shear between crust and mantle.

attractive explanation for the extension discrepancy as it implies that the measurements of crustal thinning and of upper crustal extension are both correct. The best known model is asymmetrical simple shear (Wernicke 1985): if the lithosphere was pulled apart along a single throughgoing shear zone, substantial volumes of crust would be drawn out from beneath the upper plate so that the 'upper plate' margin would be thinned more than just by extension along the visible faults, leading to an extension discrepancy. However, in this case, the controlling fault should be present on the conjugate 'lower plate' margin, where the amount of measurable extension should thus exceed that required to explain the thinning (an inverse extension discrepancy). The predominance of the extension discrepancy means that all margins appear to be upper plate margins in this model, which Driscoll & Karner (1998) dubbed the 'upper plate paradox'.

Other models for crustal DDT include lateral flow of the lower crust between more rigid upper crustal and mantle layers, e.g. with landward displacement of the lower crust (Brun & Beslier 1996), oceanward displacement of the lower crust beneath a mid-crustal detachment (Driscoll & Karner 1998), oceanward distortion of the lower crust and underlying mantle lithosphere as a result of corner flow kinematics (Kusznir *et al.* 2005; with the upper crust failing more abruptly than the deeper lithosphere) and shear of the lower crust between laterally offset loci of mantle and upper crustal extension (Coward 1986; Dunbar & Sawyer 1989; Reston 1993). As no extension discrepancy is observed at those rift basins, such as the North Sea, that are not associated with the onset of seafloor spreading, one rather uncomfortable possibility is that DDT is a process uniquely related to those rifts that eventually became oceans and, thus, that the process of continental break-up and the initiation of seafloor spreading is somehow different from that of normal rifting (Kusznir & Karner 2007).

At issue here is not whether some degree of crustal DDS or DDT occurs, as it is extremely unlikely that extension is completely uniform with depth, but rather whether crustal DDT is an adequate explanation for the extension discrepancy. To address this, I will use available geological data (samples obtained by drilling, diving and dredging), seismic velocities, results from numerical modelling and a comparison of the implications of a DDT interpretation for the extension discrepancy with the probable rheological layering of the crust and the distribution of seismicity during extension.

A basic principle in this analysis is that the volume of the continental crust cannot be changed: if the lower crust is stretched more than the upper crust in one place, it must be stretched less somewhere else; if the lower crust is removed from one place, it must be displaced to another place. An obvious counter-example of this principle is magmatic addition to the crust. As a result, I will concentrate on magma-poor

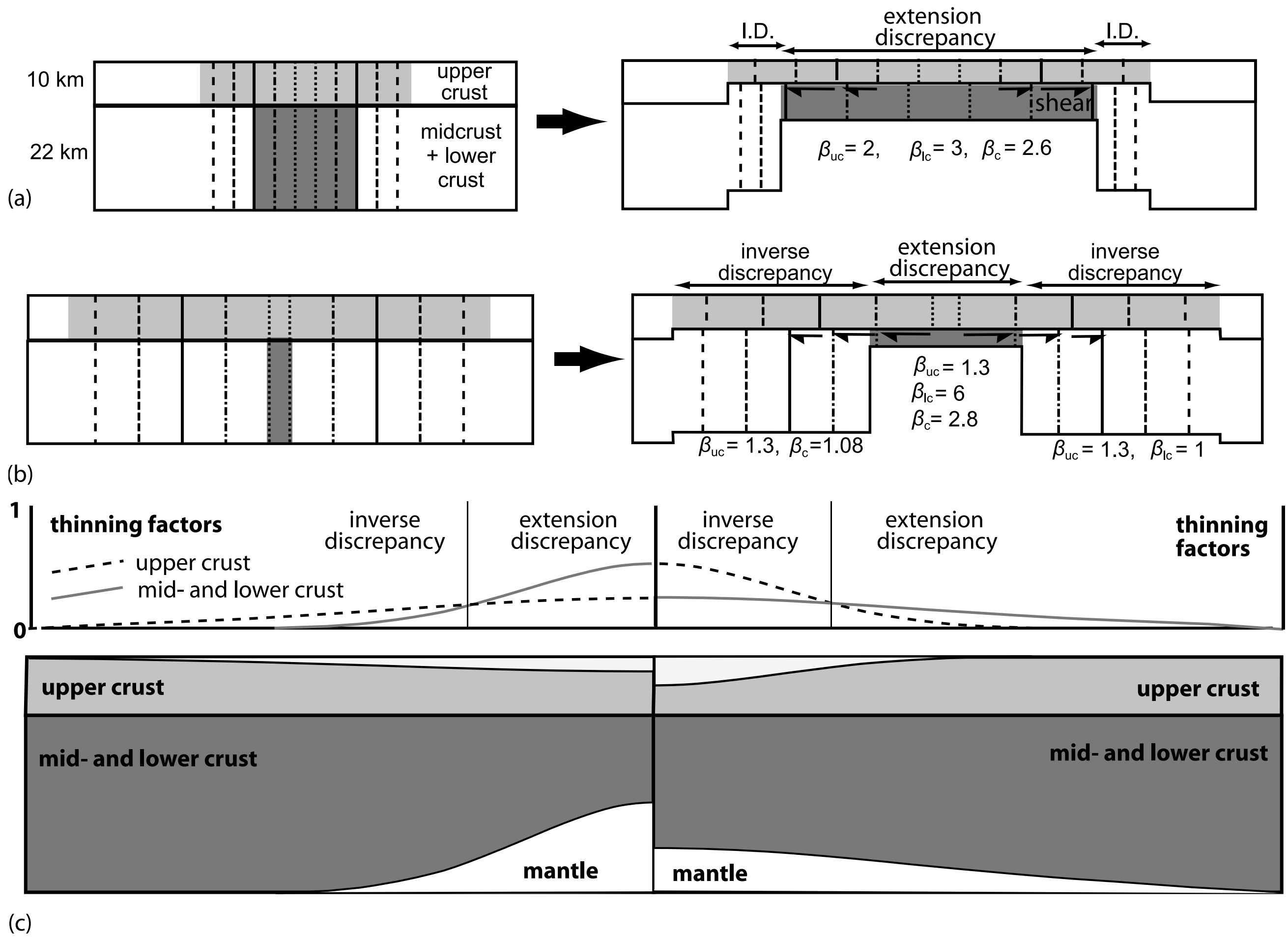

Fig. 5. Illustrations of crustal DDS and DDT. (**a**) Extension in initially 50 km and 25 km wide upper and lower crustal zones (shaded), total of 50 km extension accommodated. Much of crust develops a minor extension discrepancy (β_{lc}=3, β_{uc}=2), but an inverse discrepancy (I.D.) flanks the basin (β_{lc}=1, β_{uc}=2). Note offset of passive markers as lower crust is displaced relative to the upper crust. (**b**) Deforming upper crustal and lower crustal zones initially 100 km and 6 km wide, total of 30 km extension accommodated. Note that in the centre of the basin an extension discrepancy develops comparable to that observed at the margins. However, this model predicts that wide flanking regions should show an inverse discrepancy, which is not observed. (**c**) More continuous model in which thinning varies smoothly but is distributed differently in upper and lower crust: left – upper crustal extended and thinned over a broader region than deeper crust, but with a reduced axial thinning factor; right – opposite case. Note that in each case an extension discrepancy has to be balanced by an inverse discrepancy.

margins where the amount of igneous addition is volumetrically insignificant. However, as similar extension discrepancies exist at both magma-poor and magma-rich margins, the conclusions from the analysis may apply to all rifted margins.

An implication of the constant-volume assumption is that to balance the places where the upper crust is extended less than the whole crust, there must be others where the upper crust appears more extended than the whole crust. Consider, for example, a simple model in which the zone to be affected by extension is wider in the upper crust than in the mid and lower crust (Fig. 5). For a given and constant amount of extension, at the rift axis β_{uc} is less than β_c or β_{lc}, giving rise to an extension discrepancy. However, at the flanks of the rift, the upper crust has been extended although the underlying middle and lower crust has not: here the amount of fault-controlled extension is likely to exceed the overall thinning, giving an inverse discrepancy. As the discrepancy between whole crustal and upper crustal extension increases, so must the dimensions of the region with the inverse discrepancy (cf. Fig. 5a and b).

A second issue is the distribution of strain away from the axis: simple models that involve a constant strain from the rift axis to the edge of the deforming region require major strain discontinuities at the edge of the deforming region. More appropriate may be models in which strain increases towards the rift centre more gradually. For instance, White & McKenzie (1988) modelled the variation in strain and thinning between the crust and mantle using two different Gaussian distributions of thinning to represent the necking of the different lithospheric levels. In both cases, excess thinning of one lithospheric level in one place requires either excess thinning of the remaining lithosphere elsewhere or the displacement of the thinned volume to some other part of the section. The same sort of approach can be applied to strain at different crustal levels (Fig. 5c). Note also that these models imply considerable lateral shear between the different crustal levels: a moderate amount of either crustal or lithospheric DDT may contribute to the development of seismically reflective shear fabrics in the lower crust (Reston 1988).

All of these models require inverse discrepancies to balance extension discrepancies, but at no margin does the measured amount of upper crustal extension significantly exceed that of the rest of the crust; at no margin has a balancing inverse discrepancy been reported. (This might result from an underestimation of the amount of upper crustal extension, discussed more below.) Instead, it is generally reported that the region of upper crustal extension is no wider than that of lower crustal extension and thinning, yet β_{uc} is far less than β_c. As the excess thinning and extension of the lower crust must still be balanced somehow, several authors have proposed a net displacement of lower crustal material either oceanward (Driscoll & Karner 1998) into the COT or landward underneath unthinned crust (Brun & Beslier 1996). Inverse discrepancies might thus not be recognized as such, instead appearing either as a wide COT zone or as a thickening of the crust landward.

To appreciate the problems in hiding such displaced crust and the resulting inverse discrepancies, it is useful to illustrate the degree of crustal DDT that would be required to explain the extension discrepancy. Taking the Galicia Bank example explored by Davis & Kusznir (2004), the observed β_f (β from faults) is much lower than β_c (whole crustal stretching factor) over more than 100 km. If β_f does represent the entire extension of the upper crust, it is possible to deduce the maximum possible thickness of the brittle upper crust as nowhere can it be greater than that of the whole crust. Using the range of values for β_f and β_c determined by Davis & Kusznir (2004), it is possible to place upper and lower bounds on the thickness of the brittle upper crust, if $\beta_f = \beta_{uc}$. In both cases, the upper crust remains at an almost constant thickness, while the remaining 25 km or so of the crust thins dramatically oceanward. For Goban Spur, the brittle upper crust would be 5.5 ± 2.5 km thick; for Galicia Bank 3 ± 3 km thick. These dimensions are far thinner than the shallow seismogenic zone in regions of normal faulting (seismicity peaking at *c*. 8 km and extending down to 14 km – Jackson 1987), although it should be noted that these regions are characterized by far thicker crust than the deep margins. Constraints on the expected thickness of the brittle upper crust throughout the evolution of rifted margins come from thermal and rheological modelling of the Galicia Banks and Goban Spur lithospheres (Pérez-Gussinyé & Reston 2001), which shows that the brittle crust should be about 10 km thick at the start of rifting and remain at approximately this value as the downward migration of the brittle–ductile transition approximately matches the thinning of the crust (Fig. 6). These rheological models match the thickness of the shallow seismogenic zone (Jackson 1987) reasonably well, and show that the likely thickness of the brittle layer throughout rifting to break-up is considerably greater than required by the Davis & Kusznir (2004) interpretation.

It is possible that Davis & Kusznir (2004) underestimated the amount of fault-related extension. The depth images of the Galicia margin, in particular, allow improved estimates of the amount of extension of the deep margin during the latest phase of faulting, giving values between 35% and 100% extension (e.g. Reston 2005; Reston *et al.* 2007; Crosby *et al.* 2009), depending on the exact location and interpretation, giving a β_f of between 1.35 and 2. Crosby *et al.* (2009), however underestimate the amount of crustal thinning, which they base on estimates of crustal thickness from old wide-angle data that identified serpentinized mantle as crust. The depth images (Reston *et al.* 2007) show that true crustal basement thickness at the deep margin (between 0 km and 30 km from the Peridotite Ridge) varies from 3 km beneath the top of the blocks and *c*. 1 km in the intervening half-graben, giving an average of *c*. 2 km. The overlying sedimentary sequences are early syn-rift, were not present at the onset of rifting and can be ignored for this calculation, so, for an initial crustal thickness of 30 km, a whole crustal stretching factor β_c of *c*. 15 results, far more than that deduced from the fault geometries. Thus, a substantial extension discrepancy remains. Assuming that the deep margin consists entirely of upper crust, and equating β_{uc} with β_f gives a maximum initial upper crustal thickness of 4–5 km, still far less than the thickness of the seismogenic zone and less than the thickness of the brittle crust throughout the evolution of the margin (Fig. 6).

The section predicted if DDT explains the extension discrepancy shows that the upper crust remains at an almost constant thickness, while the remaining 20–25 km or so of the crust thins dramatically oceanward. Unless the missing lower crust is stranded on the conjugate margin (the unlikely 'upper plate paradox' referred to by Driscoll & Karner 1998), the lower crust must presumably have been displaced landwards or into the COT. For a margin thinned to *c*. 5 km over a distance of *c*. 100 km, but where $\beta_f \sim 1.25$, the amount of crust that must have been displaced by DDT would have a cross-sectional area of between 1500 km^2 and 2000 km^2 (Fig. 7). If displaced into the COT, the amount of displaced crustal material would be sufficient to create a 5 km thick layer over 300 km in margin-normal length. A cursory examination of the profiles in Figure 2 rules out the possibility that even tens of kilometres of displaced crust have been hidden within the COT, let alone hundreds of kilometres: the crust is very thin and probably dominated by serpentinized peridotites, not typical lower crustal lithologies. Furthermore, the idea that the lower crust might somehow be extruded like toothpaste does not tally with our understanding of rheology. Hopper & Buck (1996) showed that for the thermal state of typical magma-poor margins, the lower crust should, at the start of rifting, be too viscous to flow substantially; Kusznir & Matthews (1988) reached a similar conclusion. Even if the lower crust was withdrawn from beneath the brittle upper crust, the accompanying pressure and temperature reductions would render it both more viscous (and hence even less likely to flow significantly) and eventually brittle, subject to faulting. The boundary between the extruding now-brittle lower crust and intact brittle upper crust would be marked by a very large offset fault, effectively accommodating the missing tens to hundreds of kilometres of extension (Fig. 7). Thus, the sort of DDT proposed by Driscoll & Karner (1998) can only be fault controlled and thus could lead only to an extension discrepancy if almost of the faulting was not recognized.

More promising might be the idea that the lower crust is hidden further landward, notwithstanding the difficulty in the large-scale displacement of a viscous mass. However, this would lead to substantial thickening of the lower crust somewhere, leading either to a pronounced inverse extension discrepancy somewhere or even the formation of passive margin mountains. For the same extension discrepancy described above, the landward displacement of the required 1500 km^2 and 2000 km^2 of crust would require the development of a mountain belt measuring, for example, 1.5 km high by 150–200 km wide, or 3 km high by 75–100 km wide. No evidence for this has ever been reported. Furthermore, the displacement of lower crust *away* from the axis of thinning is counter-intuitive: one would expect the lower crust to be driven by pressure gradients towards the axis of crustal thinning.

Kinematic models of DDT

Kusznir and colleagues tried to address the rheological and driving mechanism problems by invoking a large-scale active corner flow, commonly used to model asthenospheric flow at mid-ocean ridges, so that the lower crust does not flow away but is sheared from underneath the upper crust by the corner flow. Kusznir and others reasoned that during break-up such corner flow affected the developing margin ahead of the propagating ridge tip and effectively led to a distortion of the lithosphere either towards or away from the line of surficial break-up. As no such discrepancy is observed at those rift

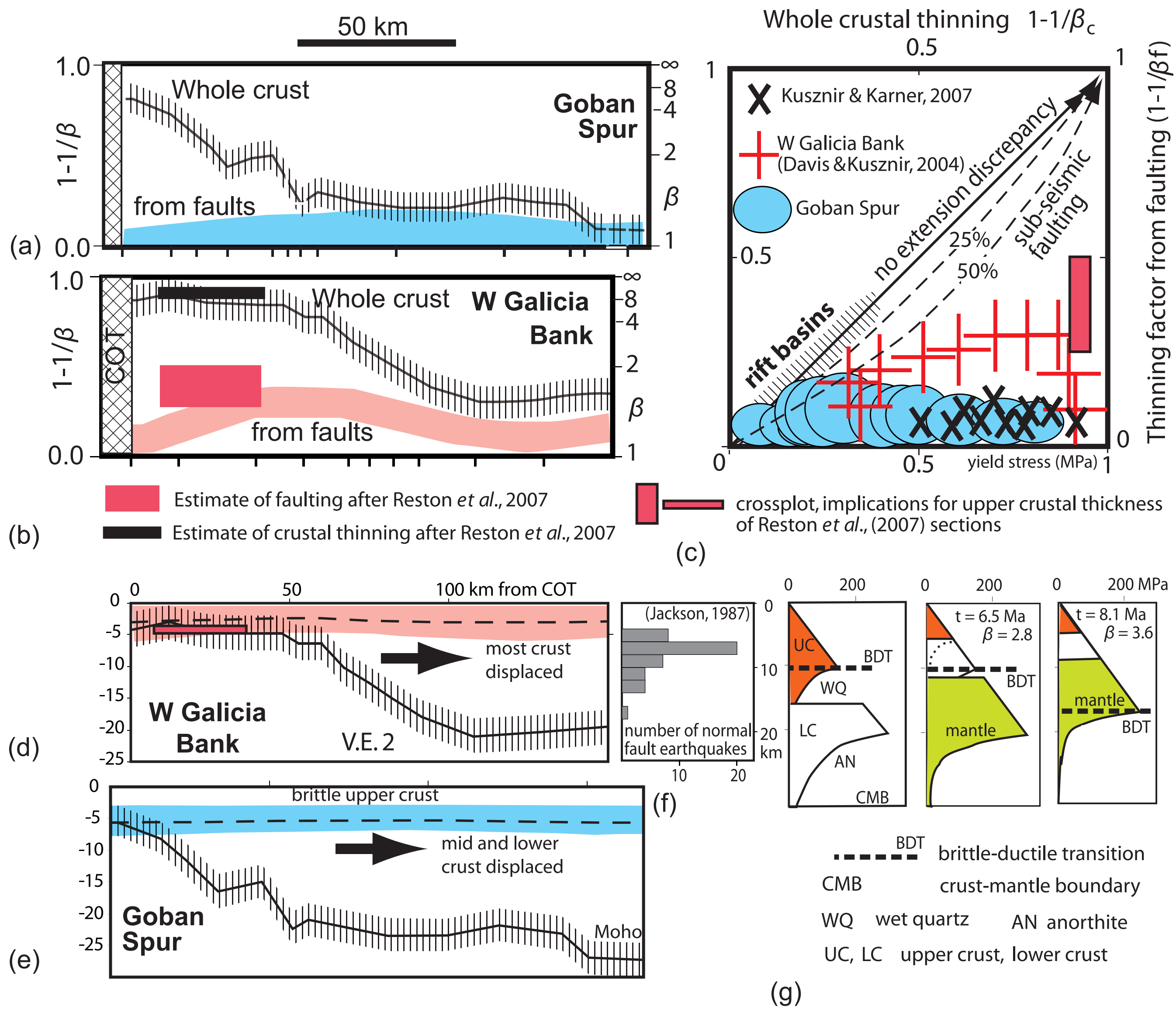

Fig. 6. Extension discrepancy and its implications. Plot of stretching and thinning factors (from faults, crustal thinning and subsidence) vs. distance from the COT for (**a**) Goban Spur and (**b**) Galicia Bank, modified after Davis & Kusznir (2004). (**c**) Cross-plot of crustal against fault-derived thinning factors: both margins plot in the bottom right quadrant, indicating a major extension discrepancy. Rectangles in (b), (c) and (d) show alternative estimates of extension and thinning, and their implications, from the latest depth section (Reston *et al.* 2007). (**d**), (**e**) Predicted crustal thickness distribution across the Galicia Bank and Goban Spur margins if the fault-measured extension presents the entire extension of the upper crust and bearing in mind that the upper crust must always be at least as thick as the whole crust. (**f**) Depth distribution of normal fault earthquakes (Jackson 1987) and (**g**) thickness of the brittle upper crustal layer at the start and during rifting (Pérez-Gussinyé & Reston 2001) for comparison. The upper crustal thickness predicted from the thinning factors is far thinner than that predicted by the rheological modelling and the thickness of the normal fault seismogenic zone. The implication is that the upper crust is extended by more than measurable from the faults. Also note that the middle and lower crust (LC) both become brittle, which would prevent flow.

basins, such as the North Sea, that are not associated with the onset of seafloor spreading, one rather uncomfortable possibility is that DDT is a process uniquely related to those rifts that eventually became oceans and, thus, that the process of continental break-up and the initiation of seafloor spreading is somehow different from that of normal rifting (Kusznir & Karner 2007).

However, these kinematic models do not actually explain the extension discrepancy. First, the volume of crust displaced from beneath the little extended upper crust is far too little (cf. Figs 8 and 7). Secondly, the models tend to predict that the displaced crust has been pushed oceanwards, as has the subcrustal lithosphere. They thus allow the unroofing of lithospheric mantle within the COT which is observed at rifted margins, but as discussed above, the same margins show that the displaced middle and lower crust cannot be hidden oceanward. By carefully selecting their parameters (Fig. 8b), Kusznir *et al.*, do manage to displace the subcrustal lithosphere slightly oceanward and the lower crust slightly landwards (resulting in local minor crustal thickening), but insufficiently to explain either the extent of mantle unroofed within the COT or the volume of crust that would need to be displaced landward to explain the extension discrepancy (Fig. 7). In short, the models provide no support for the extension discrepancy being caused by crustal DDT.

Other numerical models

The corner flow model is simply a convenient representation of asthenospheric flow at mid-ocean ridges, and not necessarily a

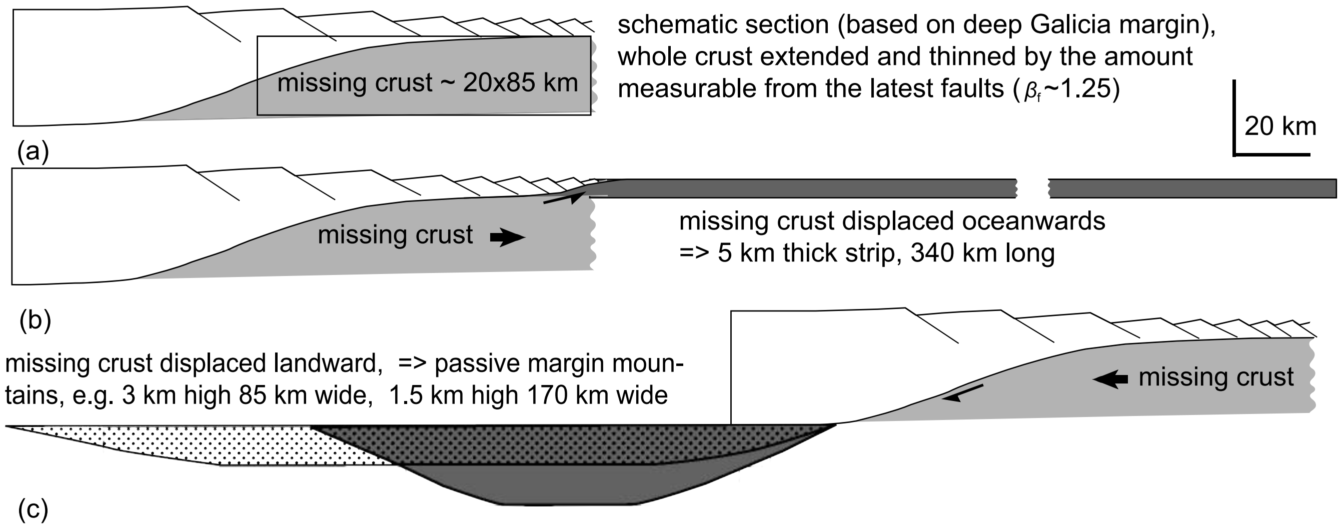

Fig. 7. Implications of crustal DDT by the lateral displacement of mid- and lower crust as an explanation for the extension discrepancy where no inverse discrepancy is observed. (**a**) If the small amount of extension measurable from the latest faults (typically <25% extension, or β_f of 1.25 – see Fig. 3) is the total amount of stretching and thinning undergone by crust that has thinned to *c.* 5 km thickness, a large cross-sectional area of the crust (light shading) would have to be removed by some other means. (**b**) Extruding it oceanwards (Driscoll & Karner 1998) would produce a 5 km thick strip, 340 km wide (dark shading) and would require a brittle fault along its top surface (as even the deepest crustal rocks are brittle as they are exhumed). (**c**) Displacing it landwards would lead to crustal thickening by, for instance, a mean of 20 km over 85 km (dark shading), or a mean of 10 km over 170 km (stipple), producing passive margin mountains 3 km or 1.5 km high, respectively. No such passive margin mountains or lower crustal extrusions have been observed.

true representation of the kinematics – let alone the dynamics – of seafloor spreading. Their relevance to lithospheric deformation at rifted margins is unclear. As a result, it might be considered more appropriate to consider numerical models where the kinematics of extension are not user-defined, as these may represent a more objective assessment of lithospheric strain. The models (Fig. 9) have the advantage over real sections that the amount and distribution of extension and thinning are known, allowing comparison with the amount of resolvable faulting (Fig. 3). Various models have been published, but here I focus on just two recent results: Lavier & Manatschal (2006) and Weinberg *et al.* (2007), both of which incorporate strain-softening, Weinberg *et al.* (2007) explored the extension of a Variscan crustal model, perhaps similar to West Iberia, 30 km thick with a 20 km quartz-dominated upper crust and a 10 km thick feldspathic lower crust above mantle (olivine). Their model showed generally fairly uniform thinning (Fig. 9a): at the edge of the model stretching factors for the upper and whole crust were 3.5 and 3.33, respectively, and, at the centre of the rift, 8 and 8.6, respectively, i.e. close to uniform stretching and thinning. Although local DDT with a horizontal wavelength of about 20km is observed, this is due to local shear zone development and is completely insufficient to explain the extension discrepancy.

Lavier & Manatschal (2006) explored a similar model (Fig. 9b–d), but presented their results as a series of snapshots, showing how faults and shear zones both developed and, crucially, were abandoned. During early extension, one set of identifiable faults develops, accommodating nearly all the brittle extension (there is some distributed deformation equivalent to 'sub-seismic' faulting) of the upper layer in a *boudinage* manner. The presence of mild DDT, however, means that the fault-derived thinning in the basin centre (between blocks I and III) slightly exceeds crustal thinning there, giving a slight inverse discrepancy. However, as extension reaches 60 km, a second generation of faults has cut across earlier faults, and the footwall to the early faults that remain active has been strongly flexed, resulting in a major potential discrepancy ($\beta_f \sim 1.2$ rather than $\beta_f \sim 2.8$ if all heaves are correctly determined, and $\beta_c \sim 2$). Note again that if all the faults were identified, DDT would result in a slight inverse extension discrepancy as the lower crust is preferentially slightly drawn towards the centre of the rift. Only a failure to recognize all fault displacement moves the model into the lower right quadrant of Figure 3.

Continuing extension to 136 km leads to the focusing of extension along two main faults (one second, one third generation) cutting down to the left. The extent of the exposed footwall is 20 km for one and 80 km for the other. In both cases, the footwall has flexed to sub-horizontal and is unlikely to be recognized as an exhumed slip surface: this can be described as 'top basement faulting' (Lavier & Manatschal 2006). Depending on the amount of faulting that may be reasonably identified, fault-derived extension β_f is likely to be between *c.* 1.2 and about 1.3, but a long way below both the true value of upper crustal extension that would be measured if all the faults were interpreted (β_{uc} and $\beta_c \sim 4.5$).

Both these sets of models show far too little crustal DDT to explain the extension discrepancy, although both show local DDT due to the development of faults and shear zones. The Lavier & Manatschal model also demonstrates that faulting follows a complex polyphase evolution and that if not all the faults are recognized, a major extension discrepancy will result, as discussed further below.

Determining the extent of crustal DDT from seismic velocities

A final test whether crustal DDT provides an explanation for the extension discrepancy comes from the seismic velocity structure of the crust. The margins shown in Figure 2 were all produced by a combination of high quality deep seismic reflection profiling and wide-angle profiling using closely spaced ocean bottom seismometers (OBS)/hydrophones and a towed seismic source. The combination of multi-channel seismic (MCS) and wide-angle data provides the best possible constraints on the velocity structure of the crust. My approach here is to relate that velocity structure to different crustal layers

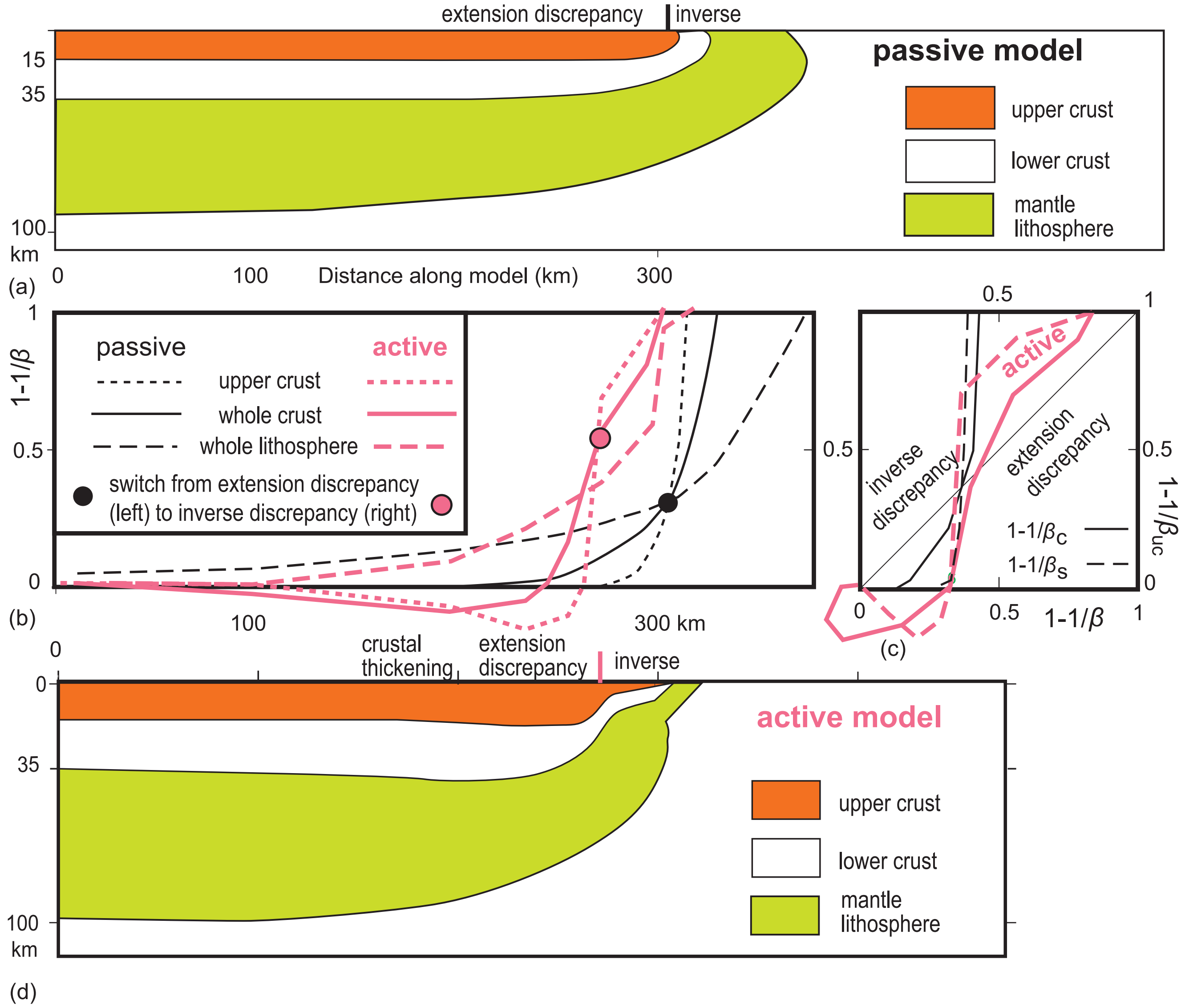

Fig. 8. (**a**), (**d**) Lithospheric DDT models (Davis & Kusznir 2004), produced by passive and active divergent flow fields, and the variation (**b**) in upper crustal, whole crustal and whole lithospheric thinning factors across them. (**c**) Cross-plot of upper crustal vs. whole crust/lithospheric thinning factors – neither model plots in the lower right quadrant and so neither model can explain the extension discrepancy.

and so to observe how the different crustal levels thin as the feather edge of the continental crust is approached.

There are some, not inconsiderable, problems with the use of seismic velocities to infer crustal type or level. First and foremost is the incorrect assumption that the velocity of any given rock is not affected by extension: velocity is, indeed, affected by fracturing, alteration and changes in temperature and pressure. However, the effects of drops in temperature and pressure tend to cancel each other out, whereas fracturing and alteration both lead to a reduction in seismic velocity. The implication is that the apparent thickness of the upper crust (based on the seismic velocity) towards the feather edge of the crust may be greater than the thickness of the thinned upper crustal layer, leading to a possible underestimate in the upper crustal stretching and thinning factors and, hence, an overestimate in crustal DDT. The second assumption is that the volumes (areas in cross-section) of the upper and lower crust remain constant during extension, a problem if substantial magmatic addition has occurred. Furthermore, as mafic intrusions would also alter the velocity structure of the intruded crust, magma-rich margins are in breach of the first assumption (velocities not modified). Consequently, the analysis is restricted to magma-poor rifted margins where the amount of igneous addition is minimized.

The velocity structures in Figure 2 provide a simple test for DDT: the thinning factor curves for the whole crust and upper crust can be plotted against each other. If there is significant DDT there should be a systematic deviation away from the diagonal: if the DDT is a possible cause of the observed extension discrepancy, the data should plot in the lower right quadrant. All ten rifted margins that provide sufficient control from the shelf to the COT plot close to the diagonal (Fig. 10). Although several show some evidence for local DDT (e.g. SCREECH 3 or Labrador, where upper crust appears to continue out over serpentinized mantle), the upper crust is also very strongly thinned so the data plot in the top right rather than the bottom right quadrant and the DDT is insufficient to explain the extension discrepancy.

The possible problems in using velocity structure to infer the thinning of different crustal levels do not help, as the general effect of rifting would be to reduce velocity through fracturing and alteration, thus giving lower crustal rocks an

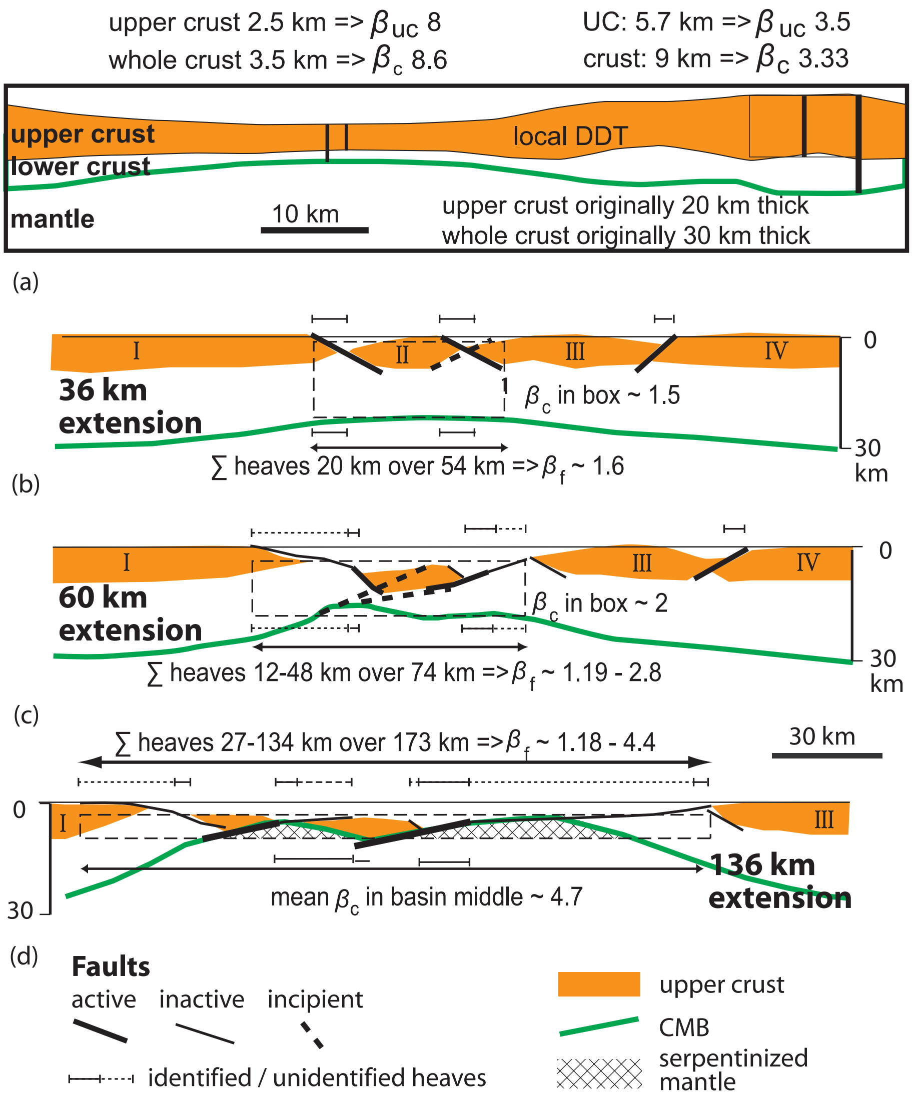

Fig. 9. Crustal structure produced by dynamic numerical models. (**a**) Weinberg *et al.* (2007). Although there is some excess thinning and lateral displacement of the lower crust, it is far too little to produce a significant extension discrepancy. (**b**)–(**d**) Model of Lavier & Manatschal (2006) at different amounts of extension. Local DDT is controlled by parting of upper crust along faults, but there is little large-scale displacement of the deep crust. If only some of the faulting is recognized, there is a major extension discrepancy ($\beta_c \gg \beta_f$), but not if faults are completely identified. See Figure 3. CMB, crust–mantle boundary.

upper crustal velocity and meaning that the thin upper crustal layer, such as observed on SCREECH 3, may actually be lower crustal rocks, as was found by ODP legs 149 and 173. These legs drilled a series of wells across the highly thinned crust of the west Iberia margin, sampling crustal blocks with seismic velocities generally well below 6.5 km s^{-1} (Chian *et al.* 1999), but recovered at Site 1067 and 900 amphibolites, anorthosites and mafic granulites, i.e. typical mid-crustal to lower crustal rocks (Whitmarsh *et al.* 2000) exhumed in the toe of fault blocks that were rotated to horizontal. The mafic granulites/amphibolites passed through the hornblende-blocking temperature for argon (500°C) at *c.* 161 Ma and the plagioclase-blocking temperature (150°C) at 136 Ma, indicating that they were in the deep crust before the start of rifting and almost fully exhumed 25 Ma later (Tucholke *et al.* 2007). As these sites are flanked by recoveries of upper crustal sedimentary units, the displacement of the lower crust into the COT can also not be invoked in this case: the exposure of lower crustal rocks is the result of complex polyphase faulting and block rotation.

The plot in Figure 10 only covers the ten conjugate margins where the velocity structure can be traced far enough landward to estimate the relative thinning of the crustal layers. However, the sort of DDT required to explain the extension discrepancy (Fig. 3) is also unlikely to apply at several other margins as these exhibit velocities just above the crust–mantle boundary (CMB) that are comparable with these ten. For instance, the Goban Spur section has a lower crustal layer with a seismic velocity of 7.0 km s^{-1}; Congo–Angola 6.8 km s^{-1}; the Armorican margin 6.8–6.9 km s^{-1}. (The Congo–Angola margin is interesting as the presence of little-faulted shallow-water sediment directly on top of highly thinned crust has been interpreted as strong evidence for DDT with most of the crustal thinning occurring after deposition and without significant upper crustal extension.) Indeed, none of the margins where the velocity structure has been determined by modern OBS data reveals any evidence for significant crustal DDT.

In summary, there is no evidence that the extension discrepancy is caused by crustal DDT at any of these margins. Crustal DDT on the scale required to explain the extension discrepancy is not predicted by numerical modelling and is not compatible with the velocity structure of rifted margins. Crustal DDT on the scale required to explain the extension discrepancy is not compatible with either the initial or the evolving rheology of the crust, nor with the depth distribution of normal faulting earthquakes. Crustal DDT on the scale required to explain the extension discrepancy would, in the absence of extensive inverse discrepancies, require either massive oceanward or landward displacement of most of the crust from beneath the little faulted uppermost crust: the implied inverse discrepancies, passive margin mountains and lower crustal extrusion are neither observed nor likely. In short, crustal DDT cannot explain the extension discrepancy.

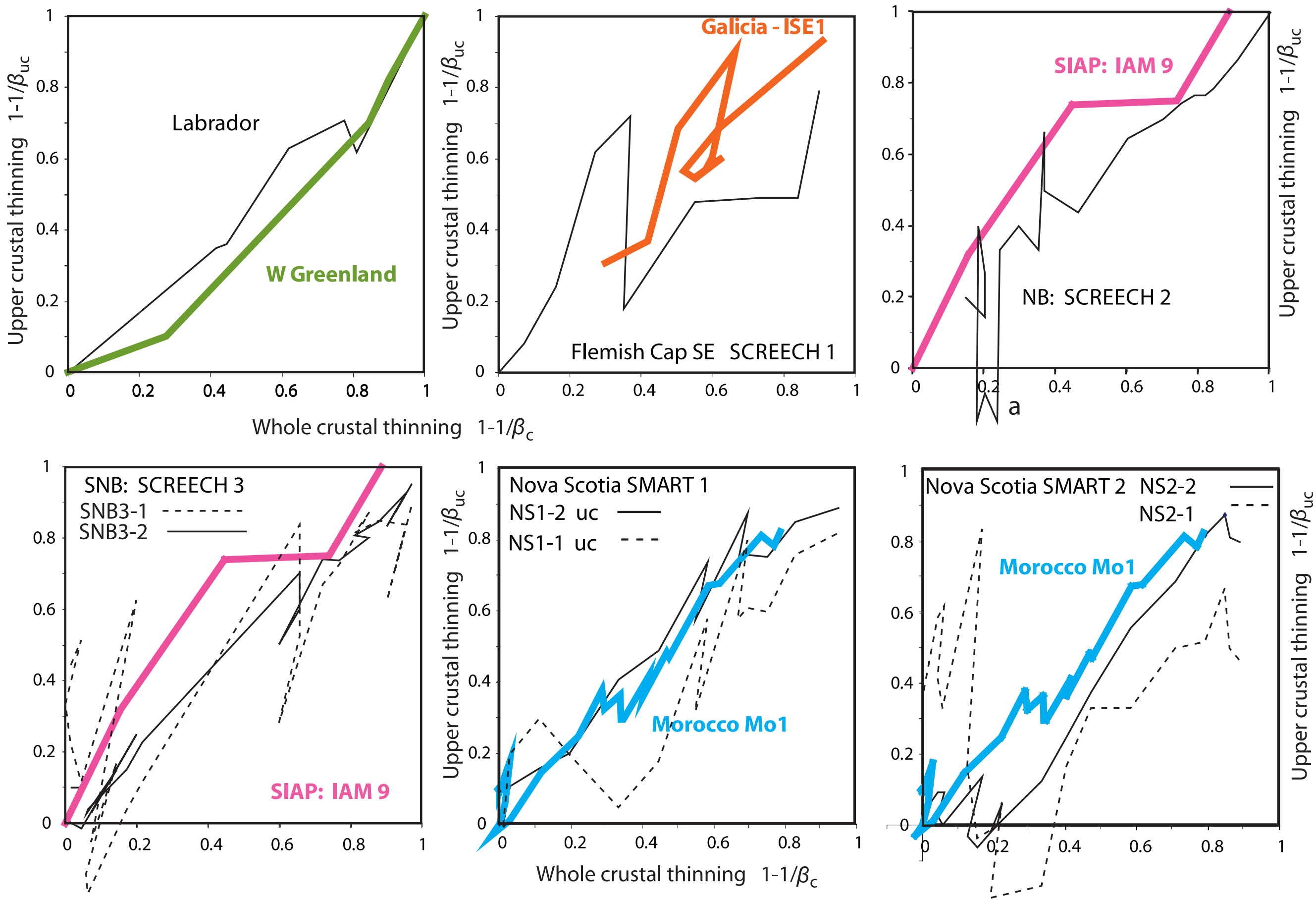

Fig. 10. Cross-plot of upper crustal vs. whole crustal thinning factors (for conjugate margin pairs) derived from velocity boundaries or contours marked in Figure 2. All plot approximately along the diagonal, indicating only local, fault-controlled crustal DDT, even when a thin upper crustal layer is defined. The implication is that there is little crustal DDT so it cannot explain the extension discrepancy.

UNRECOGNIZED EXTENSION

We have seen that crustal DDT cannot explain the extension discrepancy as $\beta_{uc} \sim \beta_c$. As the extension discrepancy means $\beta_c \gg \beta_f$, the implication is that $\beta_{uc} \gg \beta_f$, i.e. we may not be measuring all the extension. To understand why this might be the case, we need to consider how we measure extension.

Extension of the brittle crust occurs through displacements along normal faults. As the faults accommodate extension, the horizontal length of the fault blocks is increased by a combination of the development of fault heave, the rotation of the blocks and their internal deformation. As discussed above, the internal deformation is hard to quantify but alone is unlikely to explain the extension discrepancy, although it undoubtedly contributes to it. Block rotation alone would actually lead to negative extension and simply allows the development of large offsets along faults without the development of very rugged topography (Jackson 1987). Thus, if we are dramatically underestimating the amount of extension, we must be somehow underestimating the amount of fault heave.

Identifying true pre-rift

The correct identification of fault heave depends on the identification of a continuous pre-rift marker horizon on both sides of the fault. Generally, this is the pre-extension top of the crust, typically a pre-rift sequence, although in terranes that were originally above sea-level before rifting, the pre-rift crust may consist entirely of basement rocks. However, on seismic data in particular, we cannot distinguish between any sub-crop of top basement beneath the post-rift or syn-rift and the top of the pre-rift crust unless a true pre-rift sequence is identifiable, the marker horizon. Identification of a true pre-rift sequence is problematic as the main criteria are continuity, close-to-parallel bedding and shallow-water deposition. The danger is that any more or less continuous unit, offset only by minor faulting, may be interpreted as pre-rift even if it was deposited after considerable extension. For instance, units deposited during thermal subsidence (post-rift) to an early phase of rifting would exhibit all the characteristics of a deposition during a sag phase prior to a later phase of faulting. Although in places thickness variations might indicate that the sequence is not truly pre-rift, downward-thickening units will become more constant in thickness as the deeper parts of the sequence undergo greater compaction. This effect is exacerbated by the tendency to work with time sections: downward-increasing compaction resulting in downward-increasing seismic velocity, and hence downward-decreasing interval times for a given thickness.

It might be argued that such units should be distinguishable by either deposition in moderate water depths or by the presence of underlying tilted syn-rift units, but, as is discussed further below, the use of palaeo-water depth estimates to infer subsidence (or lack of) and of subsidence to infer extension is fraught with dangers. Original syn-rift wedges are also likely to be very difficult to recognize if the margin is subsequently extended along a new array of faults. A classic example of this is the Triassic rift beneath the western flank of the north Viking Graben. Here the Late Triassic formations show gentle thickening consistent with deposition in a sag basin, but Tomasso

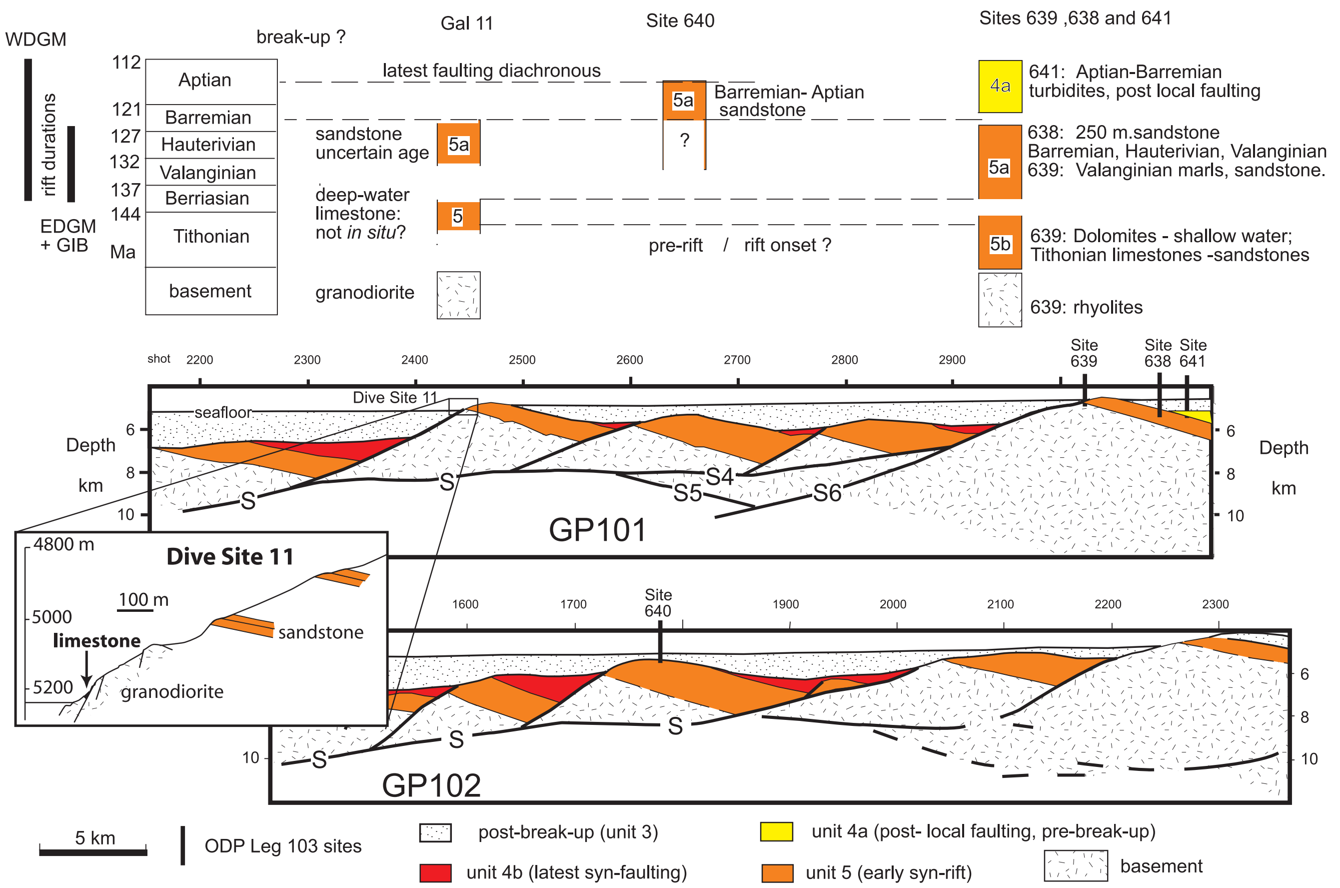

Fig. 11. Summary of drilling and diving results across the thinned continental crust west of the Galicia Bank. The seismostratigraphic units are diachronous, e.g. compare age of Unit 5 – deep-water sediment rotated within fault blocks), consistent with polyphase faulting (faulting episodes shown by dashed lines). Inset: results of Dive Site 11 of the Galinaute cruise – deep-water laminated limestones were recovered in a pocket on the fault scarp rather than on the back-tilted top of the fault block, indicating a complex (polyphase?) structural evolution. Sediments tilted on the back of the blocks may be considerably younger. EDGM, eastern Deep Galicia Margin; GIB, Galicia Interior Basin; WDGM, western Deep Galicia Margin.

et al. (2008) present convincing evidence that these were syn-rift deposited in half-graben bound by faults dipping in approximately the opposite direction to the later Jurassic faults. Similar geometries have also been inferred at the edge of the Erris Trough (Cunningham & Shannon 1997). However, in other settings, less well controlled by well data and dense seismic coverage, the early syn-rift sequences might be interpreted as true pre-rift and used to calibrate the entire extension and thinning of the crust.

It may also be dangerous to assume that apparently parallel-bedded units observed in adjacent blocks are the same age everywhere. For instance, at the Galicia margin (Fig. 11), the Barremian–Aptian units drilled within a tilted block at Site 640 were interpreted not as pre-faulting units tilted within that block but as a pocket of syn-rift or even post-rift strata deposited within a hollow on the back of the block (Mauffret & Montadert 1988) because syn- or post-faulting sediments of the same age had been drilled further east and it was assumed that pre-rift, syn-rift and post-rift ages were the same across the margin. Removing this assumption restores the sequence drilled at Site 940 to syn-rift sediments that predate the latest faulting to have affected that block, but requires that the units capping the fault blocks are very diachronous.

Further west at Dive Site 11, pockets of Tithonian deep-water marls (‘laminated limestones’) were interpreted as the equivalent of the Tithonian shallow-water limestones sampled on the back of the fault blocks at the eastern end of the section, an interpretation compatible with one age of rifting across the margin. However, the Dive Site 11 marls were not located on the back of a fault block, where they might form a continuous pre-faulting sequence like the limestones to the east, but rather in pockets on the highly fractured western scarp of the fault block (Fig. 12), requiring a more complex history of faulting and/or that the marls were reworked. The units on the back of the fault (the more gently east-dipping slope) were, in contrast, poorly dated but likely Valanginian–Hauterivian or even younger.

The problem is that interpretation is often steered not by what can be seen but by what the interpreter expects to see (Bond *et al.* 2007). For instance, there is a tendency to pick a pre-faulting unit through the top of every fault block, possibly a valid approach in areas like the North Sea where there has only been limited extension, but risky at rifted margins where the amount of brittle extension might be expected to be far greater. If polyphase faulting and/or top basement faulting is present, many fault blocks need not exhibit pre-faulting units. On the much published Lusigal 12 (Krawczyk *et al.* 1996 – Fig. 12), sediment can be imaged in places on top of the fault blocks and has been drilled and dated as Tithonian muds (not shallow-water limestones as commonly assumed for the Tithonian west of Iberia) deposited in water depths variously described as relatively deep (Shipboard Scientific Party 1994), <200 m (Collins *et al.* 1996) and turbidites below wave base (Shipboard Party 1998; Concheryo & Wise 2001). Evidence for reworking of shallow-water sediments to deeper water may explain some of the confusion (Shipboard Party 1998).

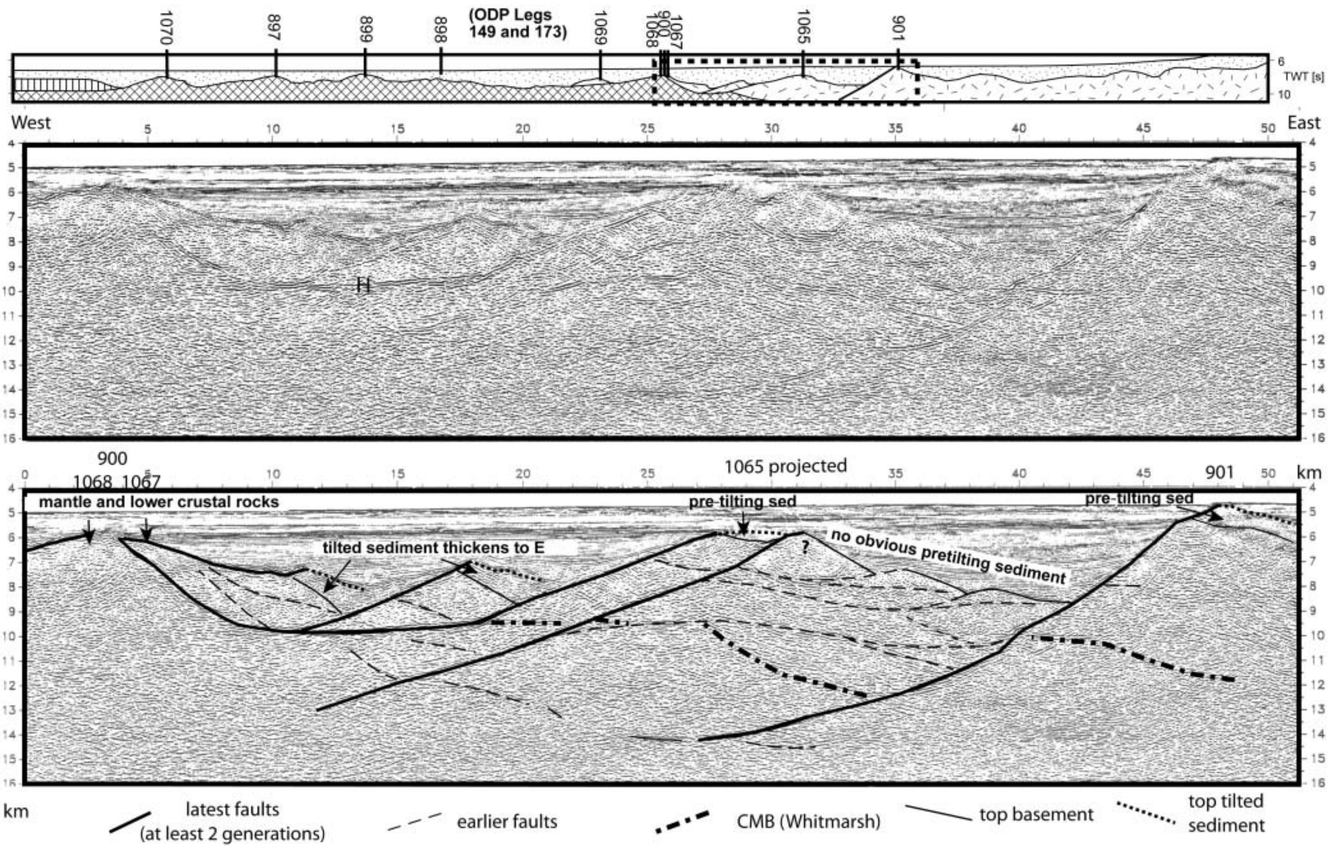

Fig. 12. Depth migration of Lusigal 12 (Krawczyk *et al.* 1996) across the Iberia Abyssal Plain margin, revealing true structural geometries. Note that multiple faults can be identified. Also note that pre-tilting sediment (*c.* 800 m depth of deposition) is imaged only locally, although it has a pronounced reflection character. It may not be present at the top of some of the fault blocks, indicating that the pre-tilting sequence may have been dismembered by several phases of faulting. CMB, crust–mantle boundary.

However, between the isolated drill sites, the sequence cannot be identified on the seismic data and the post-rift is underlain by acoustic basement (Whitmarsh & Wallace 2001), with no evidence for a sedimentary cap, let alone one of a consistent Tithonian age. Nevertheless, most interpretations assume that these are topped by a more or less continuous Tithonian sequence (Manatschal *et al.* 2001; Reston 2007*b*), placing possibly false constraints on the amount of post-Tithonian extension.

Geometry of high degrees of extension

It is clear from the discussion above that unless a genuine pre-rift sequence can be unequivocally identified across a rifted margin, the amount of extension across that margin cannot be determined accurately. Instead, the interpreter is confronted with the geometries resulting from extension with an incomplete calibration relative to the evolution of the rift. To illustrate how complex the geometry may be and how it is easy to misinterpret it and thus to underestimate the amount of extension, I now consider the evolution of the simplest possible system, a domino model. Although this is a very simple and, indeed, oversimplified model, it does illustrate the sort of structures that might result from polyphase faulting and the development of cross-cutting faults. As fault block geometries are usually recognized and interpreted on the basis of apparent pre-rift, syn-rift and post-rift geometries, it is instructive to follow these during ongoing extension.

Basic fault mechanics predict that normal faults should form at angles between 60° and 70°. In the simplest model in which the fault blocks remain internally little deformed, extension is accommodated both by slip between the fault blocks and the rotation of the fault blocks. As a result, the faults also rotate to a lower angle, remaining active due to the loss of cohesion along the fault and possibly through the development of weak fault rocks, such as clay-rich fault gouge. However, at angles below *c.* 30°, reached after *c.* 100% extension (β of 2), even weak faults should lock up, causing the extensional system to lock up. Further extension then requires the development of new faults, either cutting across the original structures or shifting the locus of extension. Such polyphase faulting has been described in several places on land (Proffett 1977; Jackson & White 1989; Booth-Rea *et al.* 2004) but, as most highly extended terranes should be under water (at rifted margins), their geometries are not familiar to many interpreters. The simplest domino model, in which the second generation of faults dip in the same direction as the first, predicts that as polyphase faulting develops (Fig. 13):

- old fault segments isolated within basement, may become increasingly hard to recognize;
- local deep basins may develop, bounded by steep-sided highs. Such basins may be starved of external sediment input, but may collect the products of mass-wasting of highly fractured basement blocks and exposed early syn-rift sediments;
- faulted exposures of syn-rift sediments are likely to be subject to reworking and mass-wasting, leading to the partial destruction of early syn-rift geometries;
- fault surfaces intersect at approximately 30°;

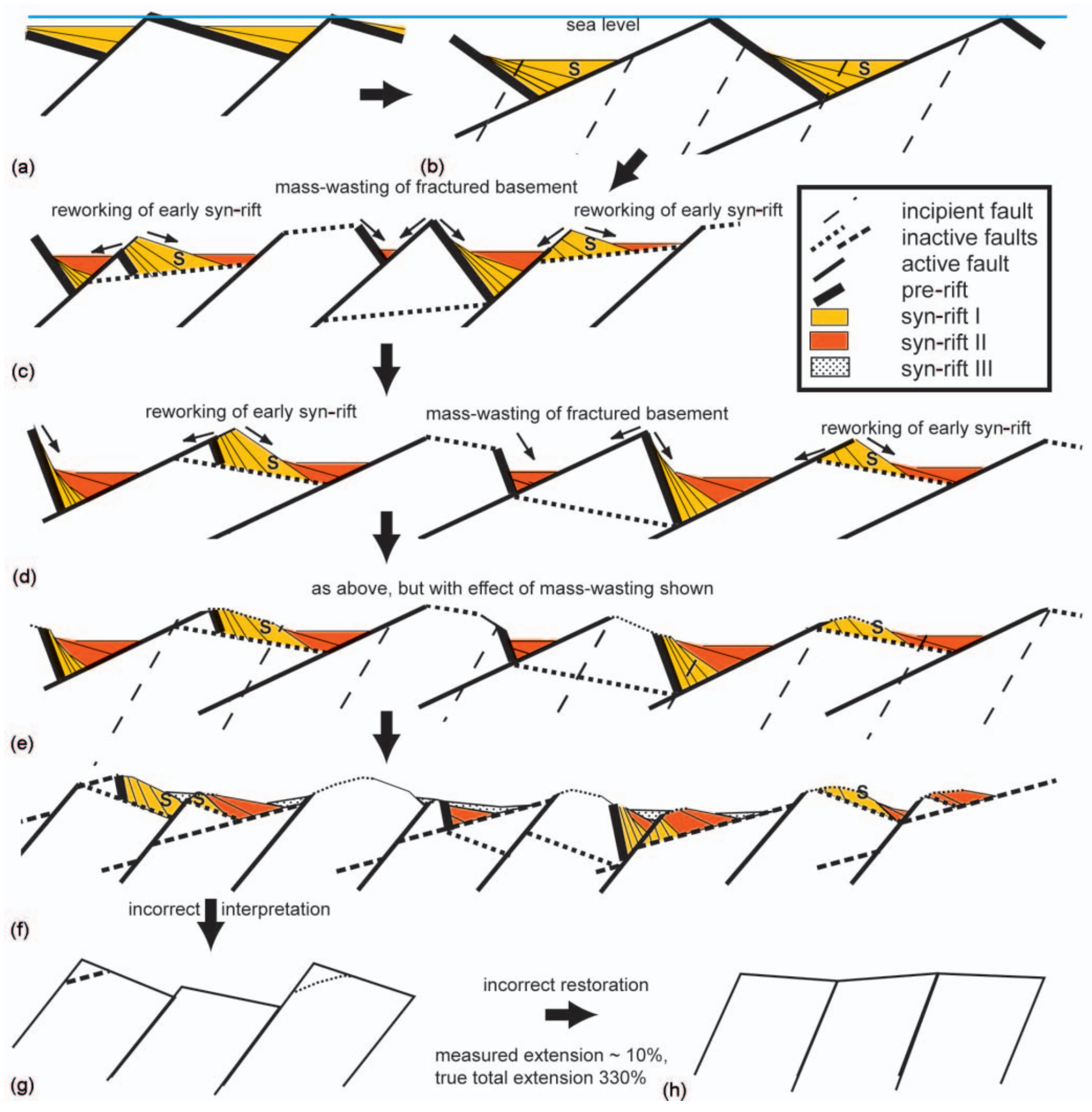

Fig. 13. Illustration of the complex geometries predicted by polyphase faulting for a simple domino model. (**a**) 25% extension, resulting in deposition in half-graben. Fault block tops emergent. (**b**) At 100% extension (stretching factor of 2), deep-water half-graben become connected as fault-block tops submerge (Barr 1987). Deposition of restricted graben facies (S) ends, original faults lock-up, new ones form. (**c**) 160% extension, early geometries dismembered by later faults, rugged fault-block topography develops, subject to mass wasting. (**d**) 300% extension, mass wasting continues. Second phase faults now rotated to *c.* 30° and lock up to be replaced by third generation faults. (**e**) as (d) except fault-block topography steeper than 30° (basement) or 15° (syn-rift) removed to simulate mass wasting. Only latest faults and blocks recognizable. (**f**) 330% extension – third generation faults have dismembered second generation faults. Continued mass wasting means that only most recent fault blocks identified, giving incorrect interpretation (**g**), which, when restored, vastly underestimates extension (**h**).

- old faults continue to dip in the original direction (but at ever lower angles) until $\beta \sim 3$; if imaged a combination of the old and new fault surfaces might be interpreted as a single phase of faulting (partly convex-up, partly concave-up), dipping at approximately 20°;
- at higher stretching factors, old faults rotate to low angles and even dip opposite to transport direction;
- second generation faults intersect the original surface at approximately 90°;
- there are steep top basement surfaces and earliest syn-rift sediments – both of which are likely to be poorly imaged;
- there is preferential reworking of the thicker portions of syn-rift sediment wedges, which are likely to occur in the footwall to the new faults. This includes much of the potential source rocks, deposited in the first generation half-graben while the fault block crests are emergent and hinder the circulation of oxygenating waters;

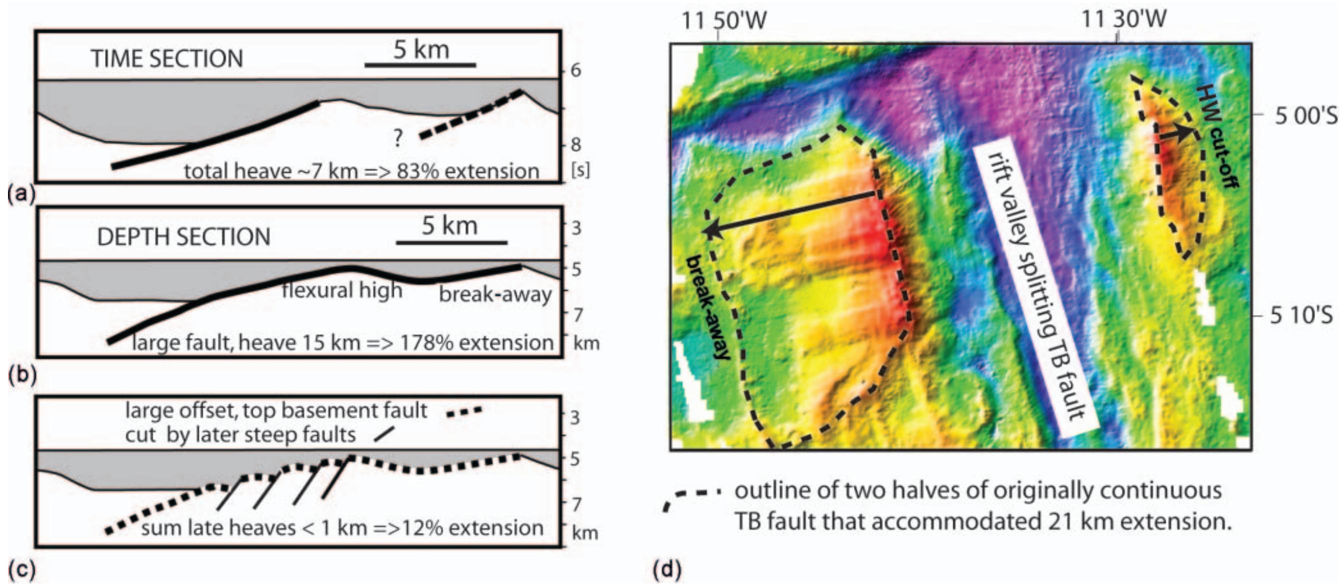

Fig. 14. Top basement (TB) fault, based on images from the Canary Basin (Reston *et al.* 2004) and from the Mid-Atlantic Ridge (Reston *et al.* 2002). (**a**) Time section: TB fault may be interpreted as two separate structures, reducing actual heave.(**b**) Depth section showing full extent of TB fault. (**c**) TB fault cut by minor faulting, e.g. accompanying flexure of footwall. Main fault not interpreted, greatly reducing measured extension. (**d**) At the Mid-Atlantic Ridge a TB fault is exposed as a corrugated surface, which has been dismembered by a ridge jump. On a seismic profile, only the latest rift and not the earlier large offset fault would be apparent. HW, hanging wall.

- true pre-rift sequences are widely scattered across the margin: sedimentary units that cap the fault blocks are various generations of syn-rift, of different ages, and cannot be used as markers to determine overall extension.

Especially when the effects of mass wasting (the gravitational collapses of the most rugged topography as mass flows of various sorts, which both remove the tops of the fault blocks and fill in the intervening basins) are included, the result is a section where the amount of extension simply cannot be determined accurately. Measuring the geometry of the fault blocks apparent after 330% extension (β=4.3) yields an estimate of only 10% extension ($\beta_f \sim 1.1$), firmly within the extension discrepancy field (Fig. 3).

Large-offset normal faulting

The domino model assumes that the blocks remain internally undeformed and that several faults are active simultaneously. A modified, ‘soft’ domino model allows some internal block deformation and for faults to be active not at precisely the same time, but produces much the same geometries. At the other extreme is a model in which only one fault is active over a long period of time. As such a fault moves, the footwall in particular must flex to prevent the development of excessive topography, and the hanging wall must flex to allow the resulting rotation of the fault.

Just as with the domino model, the rotation of the fault means that it rotates to angles too low for slip to occur. However, unlike the domino model, in which the fault remains approximately planar as the hanging wall and footwall rotate equally, the flexural rotation of the footwall means that the slip surface develops a convex-up geometry, so that the fault flattens upwards. The curvature of the fault controls the position at which the fault rotates to a sufficiently low angle for it to lock up. If this occurs above the crust, i.e. where the slip surface has been exhumed, the fault may remain active for a long time, accommodating large amounts of extension and exhuming the footwall slip surface to form top basement over considerable distances (Lavier *et al.* 1999; Lavier & Manatschal 2006).

Such geometries have become well known over the last ten years through the discovery of corrugated surface at slow-spreading mid-ocean ridges (Cann *et al.* 1997; Tucholke *et al.* 1998; Reston *et al.* 2002). These corrugated surfaces have been shown to be the exhumed slip surface of large-offset normal faults that root beneath the median valley along the ridge axis. However, their existence only became recognized through the imaging of the corrugated slip surface where it was exhumed to form top basement. If similar structures exist beneath rifted margins, the sediment cover means that such faults may well not be recognized, especially on 2D datasets. On 3D data they might be imaged as a corrugated surface, but recent observations from the SW Indian Ridge show that not all exhumed fault surfaces appear corrugated (Cannat *et al.* 2006).

On time sections, the flexural high of the exhumed footwall may be interpreted as a second fault scarp (Fig. 14), leading to an underestimation of the amount of extension (Reston *et al.* 2004). The recognition of top basement faults will be even more difficult if the fault is cut and offset by later faults (Fig. 14), even if these are relatively minor. As a result, any sub-cropping surface where there is no clear evidence for pre-rift sedimentary sequences may be a top basement fault. When top basement dips in the same way as the faults that cut it (e.g. on profile ISE17, discussed by Reston 2005), the case is strengthened as it is hard to explain such geometrical relationships unless top basement is a fault dipping in the same direction as the later faults. Similarly, if the angle between top basement and the latest faults is more than *c.* 70°, there is a good chance that top basement is an earlier fault dipping in the opposite direction to the later faults (Reston 2007*b*). Even if the fault intersects top basement at 60–70°, so that top basement may have been close to sub-horizontal when the fault developed, top basement can still be a top basement fault rotated to sub-horizontal prior to the latest phase of faulting. Only if unambiguous pre-rift sediments can be identified can it be demonstrated that no top basement fault exists.

The implication is that at large degrees of extension, most of the fault-controlled extension will not be recognized on seismic data. To identify the structures controlling the extension of the

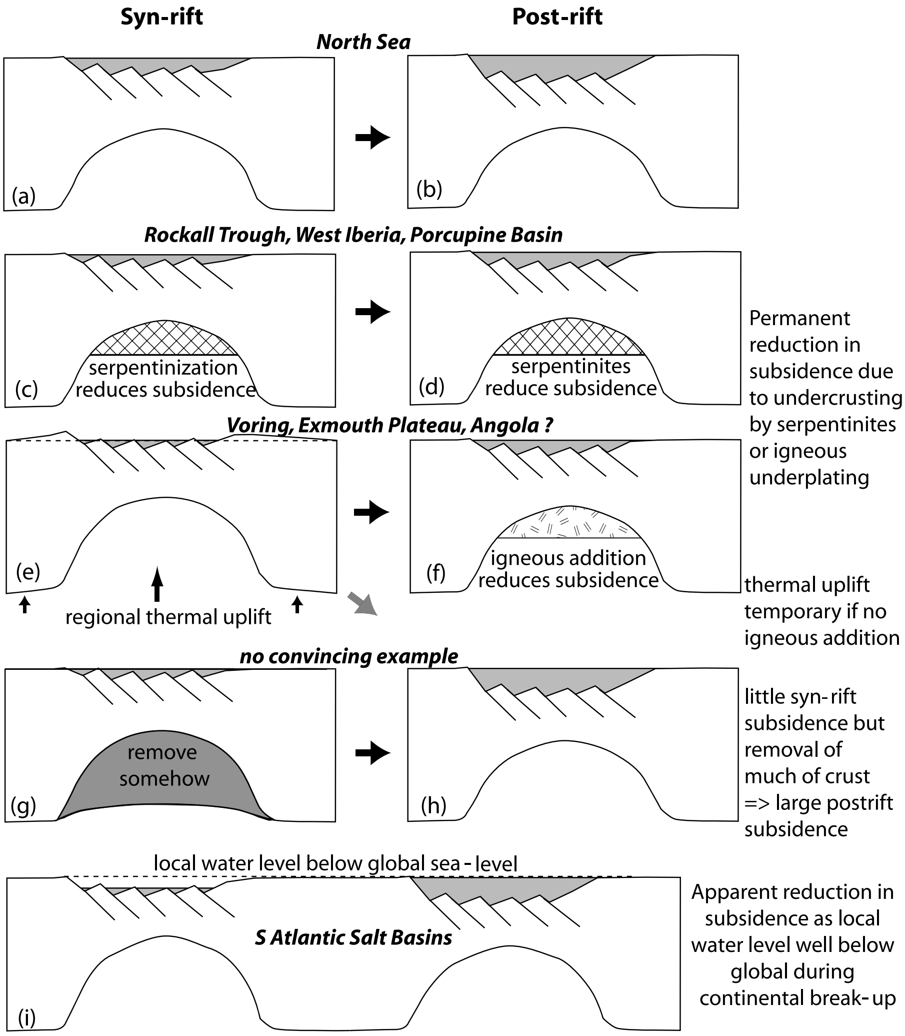

Fig. 15. Simple explanations for the syn-rift subsidence deficit (syn-rift subsidence $\ll$ post-rift subsidence). (**a**), (**b**) 'Normal' rifting with syn-rift subsidence $\sim$ post-rift subsidence. (**c**) Serpentinization during rifting converts some mantle peridotite to $\sim$ crustal density, reducing isostatic subsidence. The effect is permanent (**d**) – post-rift subsidence is normal but total subsidence is reduced. (**e**) Regional thermal uplift reduces syn-rift subsidence. The effect is temporary (reverting to (h) through excessive post-rift subsidence) unless igneous addition accompanies the thermal event, producing some permanent subsidence reduction (**f**). (**g**) Crust only slightly extended during rifting, giving shallow-water syn-rift, but then thinned without significant further rifting, e.g. by delamination or crustal DDT, increasing subsidence during early post-rift. (**h**) The mechanics of this model are problematic. (**i**) Syn-rift subsidence underestimated as local water level well below global sea-level in restricted basin (lacustrine to evaporitic deposition) formed during rifting of continental interior. True subsidence only revealed when basin connected to global ocean, appearing as excess post-rift subsidence.

brittle upper crust it will be necessary to deliberately seek structures that can be interpreted as earlier faults, requiring not only seismic data, but also carefully designed drilling campaigns, designed to sample early generations of faults, to sample multiple generations of syn-rift sediments and to determine the pre-rift structural level of the exhumed basement.

The ease with which extension can be underestimated provides a mechanism by which any inverse discrepancies associated with crustal DDT might go unrecognized; if only 50% of the brittle extension was to be recognized, places where the upper crust is stretched and thinned twice as much as the deep crust might appear not to have an inverse discrepancy. Thus, in combination with unrecognized faulting, some crustal DDT might contribute to the extension discrepancy. However, as extension is accurately measurable in rift basins and only becomes a problem at large degrees of stretching, inverse discrepancies should be recognizable. Furthermore, all other lines of evidence (deep margin geology, velocity structure, numerical models, rheology, earthquakes) are against significant DDT, suggesting that the main cause of the extension discrepancy is unrecognized faulting.

SYN-RIFT SUBSIDENCE DEFICIT

We have seen that the extension discrepancy can be readily explained by unrecognized faulting, but not by crustal DDT. A related issue is the syn-rift subsidence discrepancy: at several margins, shallow-water sediments above thin crustal basement are little faulted, yet now lie at several kilometres of water depth. The isostatic implication is that these sequences have somehow subsided by several kilometres with little extension. Leaving aside the not insubstantial errors possible in determining palaeobathymetry, this can, in principle, be explained in several ways (Fig. 15).

1. Post-depositional crustal thinning with little or no faulting

Such thinning could, for instance, include crustal DDT in which the crust is thinned through the removal of the lower and middle crust, but, as discussed above, there are serious problems with invoking crustal DDT on the scale required.

2. Buffering or delaying of subsidence during rifting and crustal thinning

Considerable crustal extension and thinning (which controls the total eventual subsidence) may have occurred before significant subsidence, so that late syn-rift or even post-rift sediments were deposited in shallow water. Syn-rift subsidence would need to be buffered in some way, for instance:

- through the presence of a thermal anomaly;
- through mineralogical and density changes in the mantle;
- by buffering through serpentinization;
- by buffering through influx of warm asthenosphere.

Thermal anomaly

A mantle plume or other excess temperature mantle anomaly provides a simple method of elevating a region during rifting so that sediments deposited immediately after rifting may be deposited in shallow water. Thermal subsidence occurs as the plume material cools and as the lithosphere thickens back towards its original geotherm. However, addition of any igneous material will result in a permanent uplift controlled by the density of the intrusion. As the depletion of the mantle also reduces its density, this will also contribute to a reduction in subsidence during rifting.

The presence of a mantle plume or similar anomaly causing thermal uplift during rifting is hard to reconcile with the formation of a magma-poor margin, such as the West Iberia margin, but may provide a simple explanation for the apparently shallow-water sequences that cover the Exmouth Plateau. Although originally considered to be a magma-poor margin adjacent to the magma-rich Cuvier Basin, the velocity structure (Fig. 2) of this margin appears to indicate classical mafic underplate. Reclassifying the Exmouth Plateau margin as a magma-rich margin implies that any subsidence discrepancy here might be related to uplift above a thermal anomaly in the mantle.

The velocity structure off Angola might also be consistent with mafic underplate: although Contrucci *et al.* (2004*a*), interpret this margin as magma-poor with undercrusting by serpentine where the crust has thinned to *c.* 5 km, a similar high velocity body occurs further landward where the crust should not be entirely brittle. This body may be original lower crust or, perhaps more likely, mafic underplate, in which case the margin cannot be considered to be magma-starved. As the margin is *c.* 1000 km from the Walvis Ridge, the Etendeka flood basalts and the Parana on the conjugate margin, it would perhaps be surprising if the margin was entirely amagmatic.

Similarly, there is good evidence of dynamic mantle support of some margins at the present day: there is a *c.* 1 km disparity in the elevation of the Newfoundland and Iberian margin for instance (e.g. Minshull *et al.* 2001). There is no reason to suppose that similar dynamic topography could not also have developed during the rifting.

Mineralogical and density changes in the mantle

As the lithosphere thins, the pressure drop causes various mineralogical changes to occur, resulting in the conversion of garnet to spinel and spinel to plagioclase. The resulting drop in density provides an uplift that, in effect, can markedly reduce subsidence by hundreds to thousands of metres (Simon & Podladchikov 2008), although it is unclear if the kinetics of the changes are rapid enough. These authors have proposed this model as an explanation for the reduced syn-rift subsidence of the Voring Plateau, although both thermal and igneous effects probably also contributed.

Uplift due to mantle serpentinization

At the West Iberia margin, the extreme lack of magmatism may indicate the presence of cool and/or depleted mantle rather than hot sub-lithospheric mantle during rifting. As a result, any subsidence discrepancy here must be explained in some other way. One possibility is mantle serpentinization. The hydration of the uppermost *c.* 6 km of the mantle once the crust has become entirely brittle leads to a drop in density and an increase in volume. The net result is that every 1 km of serpentine replacing olivine (e.g. 25% serpentinization over 4 km) leads to a permanent uplift of *c.* 320 m. For typical magma-poor margins, this corresponds to an uplift (reduction in syn-rift subsidence) of between 200 m and 1000 m.

Depth-dependent lithospheric stretching

Subsidence can also be reduced during extension if the degree of mantle thinning is greater than that of the crust. For typical lithospheric parameters, if mantle thinning is approximately twice that of the crust, syn-rift subsidence is completely buffered by the thermal uplift accompanying excess mantle thinning. However, as with all DDT, it seems likely that the excess mantle thinning would need to be buffered somewhere by a deficit of such thinning. Given the outcrop of apparent subcrustal lithosphere within the COT of most magma-poor margins, some degree of lithospheric-scale DDT is required beneath continental margins. If the mantle stretching factor β_m was greater than that of the crust β_c, this would in turn produce a component of extra thermal uplift during rifting, leading to reduced syn-rift subsidence. For instance, where β_m is 6 (90 km subcrustal lithosphere reduced to 15 km thickness) beneath crust thinned by a factor of β_c=3 (30 km thick crust reduced to 10 km), the predicted syn-rift subsidence would be reduced by close to 700 m. Such a model was proposed for the Voring Plateau (Simon & Podladchikov 2008). However, the presence of lithospheric mantle within the COT would imply a reduced thermal uplift (hence an increased syn-rift subsidence) where the crust is extremely thin (more thinning than the mantle) or absent. As a result, simple models of lithospheric DDT, although a good explanation for mantle unroofing and for post-rift onlap, are not a good explanation for the syn-rift subsidence deficit at deep margins where the crust thins to zero thickness.

Influx of warm asthenosphere

A final way that syn-rift subsidence might be partially buffered is through the influx of warmer asthenosphere as cool subcrustal lithosphere thins. Reston & Phipps Morgan (2004) described evidence that the continental sub-lithospheric upper mantle in places is cooler than a T_p of 1300°C. Rifting above such cool sub-lithospheric mantle would not only lead to significant melt suppression, but would require the influx of normal ~1300 T_p asthenosphere before true oceanic crust could form through partial melting. If this influx was to start during rifting, it would lead to a thermal uplift buffering syn-rift subsidence. As the influx might be permanent as cool subcontinental sub-lithospheric mantle is replaced by warmer oceanic asthenosphere, this uplift would be permanent, in effect.

The magnitude of the thermal uplift accompanying influx of 'oceanic' asthenosphere beneath the extending margin would depend not only on the temperature contrast between the two types of sub-lithospheric mantle, but also on the geometry and mechanism of influx. For instance, oceanic asthenosphere might intrude as a tongue at some depth below the thinning lithosphere, with little change in the thickness of the continental sub-lithospheric mantle beneath the rift, requiring complete decoupling between the lithosphere and the underlying sub-lithospheric mantle. As the lithosphere thins towards zero, this might reduce subsidence by as much as 600 m per 100 K temperature difference between the sub-lithospheric mantle and the warmer intruding asthenosphere. The other end-member would have the sub-crustal lithosphere thinning in much the same way as the overlying lithosphere as extension progresses, implying considerable coupling between the lithosphere and the underlying cool sub-lithospheric mantle. If the subcrustal lithosphere thins exactly as the overlying lithosphere,

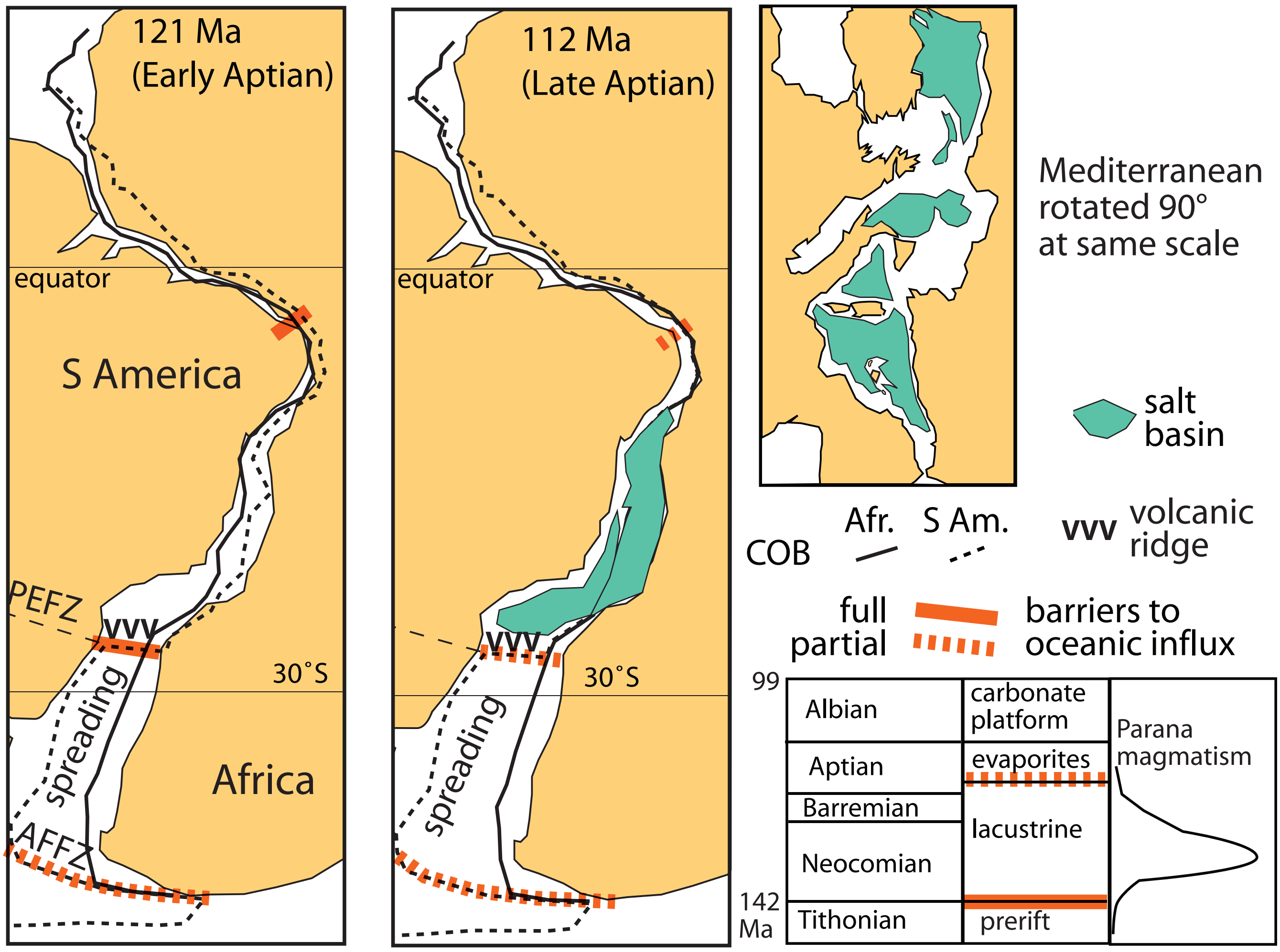

Fig. 16. Opening of the South Atlantic and deposition of the salt basin, after Torsvik *et al.* (2009). The Agulhas–Falklands Fracture Zone (AFFZ), the Parana–Etendeka FZ (PEFZ) and/or the volcanic ridges that developed in the Walvis Ridge and Rio Grande Rise may have been instrumental in preventing marine incursion from the south prior to the Aptian. Pre-Aptian lacustrine source rocks may have been deposited below global sea-level in the isolated, deepening basin. Salt accumulation replaced lacustrine conditions in the early Aptian, when the rift basin partially connected to the open ocean. The dimensions of the salt basin are comparable to that of the Messinian in the Mediterranean, believed to have formed in shallow water in a desiccating deep basin. COB, continent–ocean boundary.

the subsidence reduction as the lithosphere thins towards zero may exceed 2500 m for every 100 K temperature difference.

In summary, even away from mantle plumes, there are several mechanisms by which syn-rift subsidence may be reduced. Indeed, it could be argued that as both mantle serpentinization and the influx of warm oceanic asthenosphere beneath a cooler continent are likely to occur during rifting at magma-poor margins, that a syn-rift subsidence deficit is to be expected.

3. Deposition in a shallow-water but deep, subsiding basin

Palaeobathymetry, corrected for eustatic sea-level variations, only reflects subsidence if the basin is connected to the global ocean, otherwise water level may be quite different to global sea-level. If local water level is below global sea-level, palaeobathymetry estimates do very little to constrain subsidence and so there is very little control on the magnitude of syn-rift subsidence. Although such circumstances may not generally occur, they might when break-up starts through rifting in the interior of a continent and the rift develops with no connections to the surrounding ocean. A particular example may be the South Atlantic (Fig. 16), where syn-rift lacustrine source rocks and the overlying thick evaporite sequences both imply deposition in a setting that was not fully connected to the global ocean. Extensive evaporite sequences (saline giants) probably indicate increasing marine input into the basin, but little or no return flow, most easily explained if local sea-level was substantially below the global level, such as the Mediterranean during the Messinian salinity crisis. Immediately prior to the onset of marine influx and consequent evaporite accumulation, the same basin would probably have been completely cut-off from the global ocean and partially filled by freshwater (river) influx, giving a shallow-water deep basin lacustrine environment, where local water level was substantially below global sea-level. As a result, estimates of subsidence of this basin based on the lacustrine sediments are likely to be completely erroneous.

It is interesting to note that the dimensions of the South Atlantic salt basins are comparable to the Mediterranean at the time of the Messinian salinity crisis (Fig. 16): although the cause of basin formation was quite different; size is no obstacle to the isolation of a deep basin from the open ocean. Spasmodic influx of normal salinity seawater from the global ocean might lead to short-lived periods of normal salinity as the basin developed, but the latter do not themselves require complete connectivity to the global ocean. The barriers to seawater influx may have been the incipient Equatorial rift and transform margins in the north and the Walvis Ridge, a precursor plume swell in the south (the site of the Parana and Etendeka large igneous province or possibly the Parana-Etendeka Fracture Zone – Torsvik *et al.* 2009). Only during Barremian time did complete connectivity develop, either from the north (Bate 1999; Dingle 1999) or from the south.

IMPLICATIONS FOR PETROLEUM GEOLOGY OF HIGHLY THINNED MARGINS

We have seen that the extension discrepancy is probably caused by the expected complex structural evolution of rifted margins rather than by crustal DDT. We have also seen that there are several ways, all to be expected during rifting to break-up, to introduce a syn-rift subsidence deficit, without resorting to crustal DDT. The implications for the petroleum geology of rifted margins concern the distribution of pre-rift plays, the distribution of syn-rift sediment developed in early half-graben (cf. Kimmeridge) and the maturation history of the basin.

- *Pre-rift plays:* It is clear that if polyphase faulting has occurred, genuine pre-rift plays are likely to be scattered across the deep margins (Fig. 13). Furthermore, they are likely to have been partially reworked by mass wasting, to be in places rather steep and hence poorly imaged. All these factors will reduce their potential as reservoir rocks.
- *Early syn-rift source rocks:* Polyphase faulting will have dismembered and scattered source rocks developed at low stretching factors, and will have subjected them to local fault-controlled uplift and thus to mass wasting, reducing their preservation potential. All these factors are likely to reduce their potential as important source rocks.
- *Late syn-rift source rocks:* In the South Atlantic, the important lacustrine source rocks may have formed quite late during the rift history, in a deep basin not fully filled with water and cut-off from the global ocean. Under these circumstances, both generation and preservation of high total organic carbon may be favourable.
- *Late syn-rift plays:* Mass-wasting of basement highs and of earlier syn-rift deposits might lead to the development of local late syn-rift deposits of high porosity and permeability within the latest half-graben. As a result, a new category of play is opened up.
- *Maturation:* Late-stage thinning of the crust by crustal DDT or delamination predicts that the thickness of the upper crust – the site of most of the radioactive heat-producing isotopes – does not change significantly towards the deep margin. However, explaining the extension discrepancy through polyphase or top basement faulting requires that the upper crust has been thinned as much as the rest of the crust, leading to a subsequent reduction of crustal heat production. The maturation history predicted by the unrecognized faulting explanation for the extension discrepancy thus differs from that predicted by crustal DDT.

CONCLUSIONS

The most common explanation for the extension discrepancy and syn-rift subsidence deficit observed at most/many rifted margins is crustal depth-dependent stretching (DDS) or depth-dependent thinning (DDT) but can be shown not to apply:

- the amount of DDS (DDT) required to explain the extension discrepancy would imply that the brittle upper layer is unreasonably thin;
- the amount of DDS (DDT) required to explain the extension discrepancy would require either substantial balancing inverse discrepancies, or the displacement of large volumes of middle and deep crustal rocks oceanward or landward. None of these is observed;
- the velocity structure of rifted margins suggests that thinning towards the continent–ocean transition is distributed approximately the same for both the upper crust and the whole crust;
- both lower crustal and upper crustal rocks are found in the highly thinned crust of the west Iberia rifted margin, the only margin where basement has been extensively sampled. The lower crust is not missing, but has been incorporated into the fault blocks as the lower crust became brittle and now appears on seismic data to be upper crust.

An alternative explanation of the extension discrepancy is that not all the faulting has been recognized. This arises through a combination of subseismic distributed deformation, polyphase faulting and the development of large-offset normal faults, in which the footwall is unroofed and forms top basement (hence these are sometimes called top basement faults):

- the diachroneity of faulting and tilting at the Galicia margin requires several phases of faulting;
- polyphase faulting is expected when extension exceeds 100% (stretching factor of 2), unless a large-offset 'top basement' fault develops;
- when combined with mass wasting, polyphase faulting rapidly leads to great difficulty in recognizing earlier phases of faulting, even for the simplest 2D geometries and most predictable models;
- top basement faults are likely to be misinterpreted as original pre-rift fault block tops. However, they might be distinguishable by the lack of parallel-bedded true pre-rift atop the fault block. The tendency to force a pre-rift pick through the fault blocks may have prevented recognition of such faults;
- top basement faults are particularly likely to not be recognized where they have been cut by later, steeper extensional structures, a type of polyphase faulting.

The apparent lack of significant syn-rift subsidence has also been invoked as evidence for depth-dependent stretching. However, several other explanations exist, including:

- transient thermal uplift during rifting and/or permanent reduction of subsidence by the addition of low-density melt to the lithosphere (and the depletion of the denser minerals in the mantle). These effects are likely to be particularly important at magma-rich margins;
- thermal uplift due to the influx of warm asthenosphere beneath cool, magma-poor margins;
- the reduction of syn-rift subsidence by serpentinization, particularly at magma-poor margins;
- underestimation of the degree of syn-rift subsidence by referencing this to local water level rather than global sea-level. This problem is likely to arise when break-up begins within the middle of a continent, so that the developing rift is cut off from the global ocean. Shallow-water lacustrine sedimentation in a deep basin is then expected before the influx of seawater, followed by the deposition of thick evaporite sequences (shallow-water, deep basin desiccation) as one-way marine influx begins prior to complete connectivity with the global ocean. This model may apply to the South Atlantic.

There is no compelling evidence for large-scale crustal depth-dependent stretching or thinning and several lines of evidence against it. The extension discrepancy can be explained simply by the difficulty in recognizing – let alone measuring – all the extension; the syn-rift subsidence deficit by several processes that are to be expected during rifted margin development.

This work has benefited from fruitful discussions with a great many people, including Nick Kusznir, Garry Karner, Bill Booth-Rea, Marta Pérez-Gussinyé, Dale Sawyer, Tim Minshull, Cesar Ranero, Jonathan Turner, Gianreto Manatschal, Ken McDermott, Mark Thompson, Bruce Levell, Nicky White and James Jackson, although none is responsible for its content. Reviews by Nicky White and John Dixon helped improve the manuscript. Funding over many years by the DFG, in particular, is greatly appreciated.

REFERENCES

Barr, D. 1987. Lithospheric stretching, detached normal faulting and footwall uplift. *In:* Coward, M.P., Dewey, J.F. & Hancock, P.L. (eds) *Continental Extensional Tectonics*. Geological Society, London, Special Publications, **28**, 75–94.

Bate, R.H. 1999. Non-marine ostracod assemblages of the Pre-Salt basins of West Africa and their role in sequence stratigraphy. *In:* Cameron, N.R., Bate, R.H. & Clure, V.S. (eds) *The Oil and Gas Habitats of the South Atlantic*. Geological Society, London, Special Publications, **153**, 283–292.

Bond, C.E., Gibbs, A.D., Shipton, Z.K. & Jones, S. 2007. What do you think this is? 'Conceptual Uncertainty' in geoscience interpretation. *Geological Society of America – GSA Today*, **17**(11), 4–10.

Booth-Rea, G., Azanon, J.M. & Garcia-Duenas, V. 2004. Extensional tectonics in the northeastern Betics (SE Spain): case study of extension in a multilayered upper crust with contrasting rheologies. *Journal of Structural Geology*, **26**, 2039–2058.

Brun, J.P. & Beslier, M.O. 1996. Mantle exhumation at passive margins. *Earth and Planetary Science Letters*, **142**, 161–173.

Bullock, A.D. & Minshull, T.A. 2005. From continental extension to seafloor spreading: crustal structure of the Goban Spur rifted margin, SW of the UK. *Geophysical Journal International*, **163**, 527–546.

Cann, J.R., Blackman, D.K. & Smith, D.K. *et al.* 1997. Corrugated slip surfaces formed at ridge-transform intersections on the Mid-Atlantic Ridge. *Nature*, **385**, 329–332.

Cannat, M., Sauter, D. & Mendel, V. *et al.* 2006. Modes of seafloor generation at a melt-poor ultraslow-spreading ridge. *Geology*, **34**, 605–608.

Chian, D., Louden, K. & Reid, I. 1995. Crustal structure of the Labrador Sea conjugate margin and implications for the formation of nonvolcanic continental margins. *Journal of Geophysical Research*, **100**, 24 239–24 253.

Chian, D., Louden, K.E., Minshull, T.A. & Whitmarsh, R.B. 1999. Deep structure of the ocean–continent transition in the southern Iberia abyssal plain from seismic refraction profiles; Ocean Drilling Program (legs 149 and 173) transect. *Journal of Geophysical Research*, **104**, 7443–7462.

Clift, P.D., Lin, J. & ODP Leg 184 Scientific Party. 2001. Patterns of extension and magmatism along the continent–ocean boundary, South China Margin. *In:* Wilson, R.C.L., Whitmarsh, R.B., Taylor, B. & Froitzheim, N. (eds) *Non-Volcanic Rifting of Continental Margins: A Comparison of Evidence from Land and Sea*. Geological Society, London, Special Publications, **187**, 489–510.

Collins, E.S., Kuhnt, W. & Scott, D.B. 1996. Tithonian benthc foraminifera from Hole 901A. *In:* Whitmarsh, R.B., Sawyer, D.S., Klaus, A. & Masson, D.G. (eds) *Proceedings of the Ocean Drilling Program, Scientific Results*, **149**, 193–201.

Concheryo, A. & Wise, S.W. Jr. 2001. Jurassic calcareous nannofossils from prerift sediments drilled during ODP Leg 173, Iberia Abyssal Plain, and their implications for rift tectonics. *In:* Beslier, M.-O., Whitmarsh, R.B., Wallace, P.J. & Girardeau, J. (eds) *Proceedings of the Ocean Drilling Program, Scientific Results*, **173**, 1–24.

Contrucci, I., Matias, L. & Moulin, M. *et al.* 2004*a*. Deep structure of the West African continental margin (Congo, Zaire, Angola), between 5 degrees S and 8 degrees S, from reflection/refraction seismics and gravity data. *Geophysical Journal International*, **158**, 529–553.

Contrucci, I., Klingelhoefer, F. & Perrot, J. *et al.* 2004*b*. The crustal structure of the NW Moroccan continental margin from wide-angle and reflection seismic data. *Geophysical Journal International*, **159**, 117–128.

Coward, M. 1986. Heterogeneous stretching, simple shear and basin development. *Earth and Planetary Science Letters*, **80**, 325–336.

Crosby, A., White, N., Edwards, G. & Shillington, D.J. 2009. Evolution of the Newfoundland–Iberia conjugate rifted margins. *Earth and Planetary Science Letters*, DOI:10.1016/j.epsl.2008.06.039.

Cunningham, G.A. & Shannon, P.M. 1997. The Erris Ridge: a major geological feature in the NW Irish Offshore basins. *Journal of the Geological Society, London*, **154**, 503–508.

Davis, M. & Kusznir, N.J. 2004. Depth-dependent lithospheric stretching at rifted continental margins. *In:* Karner, G.D. (ed.) *Proceedings of NSF Rifted Margins Theoretical Institute*. Columbia University Press, 92–136.

Dean, S.M., Minshull, T.A., Whitmarsh, R.B. & Louden, K.E. 2001. Deep structure of the ocean–continent transition in the southern Iberia abyssal plain from seismic refraction profiles; the IAM-9 transect at 40 degrees 20′N. *Journal of Geophysical Research*, **105**, 5859–5885.

Dingle, R.V. 1999. Walvis Ridge Barrier: its influence on palaeoenvironments and source rock generation deduced from ostracod distributions in the early South Atlantic Ocean. *In:* Cameron, N.R., Bate, R.H. & Clure, V.S. (eds) *The Oil and Gas Habitats of the South Atlantic*. Geological Society, London, Special Publications, **153**, 293–302.

Driscoll, N.W. & Karner, G.D. 1998. Lower crustal extension across the Northern Carnarvon basin, Australia: Evidence for an eastward dipping detachment. *Journal of Geophysical Research*, **103**, 4975–4991.

Dunbar, J. & Sawyer, D. 1989. How pre-existing weaknesses control the style of continental breakup. *Journal of Geophysical Research*, **94**, 7278–7292.

Funck, T., Hopper, J.R., Larsen, H.C., Louden, K.E., Tucholke, B.E. & Holbrook, W.S. 2003. Crustal structure of the ocean-continent transition at Flemish Cap: Seismic refraction results. *Journal of Geophysical Research*, **108**(B11): Art No 2531.

Funck, T., Jackson, H.R., Louden, K.E., Dehler, S.A. & Wu, Y. 2004. Crustal structure of the northern Nova Scotia rifted continental margin (Eastern Canada). *Journal of Geophysical Research*, **109**, B09102, DOI: 10.1029/2004JB003008.

Giltner, J. 1987. Applications of extensional models to the northern Viking Graben. *Norsk Geologisk Tidsskrift*, **67**, 339–352.

Hellinger, S.J. & Sclater, J.G. 1983. Some comments on two-layer extensional models for the evolution of sedimentary basins. *Journal of Geophysical Research*, **88**, 8251–8269.

Hopper, J. & Buck, W.R. 1996. The effect of lower crustal flow on continental extension and passive margin formation. *Journal of Geophysical Research*, **101**, 20 175–20 194.

Jackson, J.A. 1987. Active normal faulting and crustal extension. *In:* Coward, M.P., Dewey, J.F. & Hancock, P.L. (eds) *Continental Extensional Tectonics*. Geological Society, London, Special Publications, **28**, 3–17.

Jackson, J.A. & White, N.J. 1989. Normal faulting in the upper continental crust: observations from regions of active extension. *Journal of Structural Geology*, **11**, 15–36.

Krawczyk, C.M., Reston, T.J., Beslier, M.O. & Boillot, G. 1996. Evidence for detachment tectonics on the Iberia Abyssal Plain margin. *In:* Whitmarsh, R., Sawyer, D. & Klaus, A. (eds) *Proceedings of the Ocean Drilling Program, Scientific Results*, **149**, 603–615.

Kusznir, N. & Karner, G. 2007. Continental lithospheric thinning and breakup in response to upwelling divergent mantleflow: application to the Woodlark, Newfoundland and Iberia margins. *In:* Karner, G.D., Manatschal, G. & Pinheiro, L.M. (eds) *Imaging, Mapping and Modelling Continental Lithosphere Extension and Breakup*. Geological Society, London, Special Publications, **282**, 389–419.

Kusznir, N.J. & Matthews, D.H. 1988. Deep seismic reflections and the deformational mechanics of the continental lithosphere. *Journal of Petrology*, Special Lithosphere Issue, 63–87.

Kusznir, N.J., Hunsdale, R., Roberts, A.M. & iSIMM Team. 2005. Norwegian margin depth-dependent stretching. *In:* Doré, A.G. & Vining, B.A. (eds) *Petroleum Geology: North-West Europe and Global Perspectives—Proceedings of the 6th Petroleum Geology Conference*. Geological Society, London, 767–783.

Lau, K.W.H., Louden, K.E., Funck, T., Tucholke, B.E., Holbrook, W.S., Hopper, J.R. & Larsen, H.C. 2006. Crustal structure across the Grand Banks–Newfoundland Basin continental margin (part I)—Results from a seismic refraction profile. *Geophysical Journal International*, **167**, 127–156.

Lavier, L.L. & Manatschal, G. 2006. A mechanism to thin the continental lithosphere at magma-poor margins. *Nature*, **440**, 324–328.

Lavier, L.L., Buck, W.R. & Poliakov, A.N.B. 1999. Self-consistent rolling-hinge model for the evolution of large-offset low-angle normal faults. *Geology*, **27**, 1127–1130.

Le Pichon, X. & Sibuet, J.C. 1981. Passive margins; a model of formation. *Journal of Geophysical Research*, **86**, 3708–3720.

Manatschal, G., Froitzheim, N., Rubenach, M. & Turrin, B.D. 2001. The role of detachment faulting in the formation of an ocean–continent transition: insights from the Iberia Abyssal Plain. *In:* Wilson, R.C.L., Whitmarsh, R.B., Taylor, B. & Froitzheim, N. (eds) *Non-Volcanic Rifting of Continental Margins: A Comparison of Evidence from Land and Sea*. Geological Society, London, Special Publications, **187**, 405–428.

Marrett, R. & Allmendinger, R. 1992. Amount of extension on "small" faults: an example from the Viking graben. *Geology*, **20**, 47–50.

Mauffret, A. & Montardet, L. 1988. Seismic stratigraphy off Galicia (Spain). *Proceedings of the Ocean Drilling Program, Scientific Results*, **103**, 13–20.

McKenzie, D.P. 1978. Some remarks on the development of sedimentary basins. *Earth and Planetary Science Letters*, **40**, 25–32.

Meredith, D.J. & Egan, S.S. 2002. The geological and geodynamic evolution of the eastern Black Sea basin: insights from 2-D and 3-D tectonic modelling. *Tectonophysics*, **350**, 157–179.

Minshull, T.A., Dean, S.M., White, R.S. & Whitmarsh, R.B. 2001. Anomalous melt production after continental break-up in the southern Iberia Abyssal Plain. *In:* Wilson, R.C.L., Whitmarsh, R.B., Taylor, B. & Froitzheim, N. (eds) *Non-Volcanic Rifting of Continental Margins: A Comparison of Evidence from Land and Sea*. Geological Society, London, Special Publications, **187**, 537–550.

Pérez-Gussinyé, M. & Reston, T.J. 2001. Rheological evolution during extension at passive non-volcanic margins: onset of serpentinization and development of detachments to continental break-up. *Journal of Geophysical Research*, **106**, 3691–3975.

Proffett, J.M. 1977. Cenozoic geology of the Yerington dsitrict, Nevada, and implications for the nature of Basin and Range faulting. *Bulletin of the Geological Society of America*, **88**, 247–266.

Reston, T.J. 1988. Evidence for shear zones in the lower crust offshore Britain. *Tectonics*, **7**, 929–945.

Reston, T.J. 1993. Evidence for extensional shear zones in the mantle offshore Britain, and their implications for the extension of the continental lithosphere. *Tectonics*, **12**, 492–506.

Reston, T.J. 2005. Polyphase faulting during the development of the west Galicia rifted margin. *Earth and Planetary Science Letters*, **237**, 561–576.

Reston, T.J. 2007*a*. The extension discrepancy at North Atlantic non-volcanic rifted margins: depth-dependent stretching or unrecognised faulting? *Geology*, **35**, 367–370.

Reston, T.J. 2007*b*. The formation of non-volcanic rifted margins by the progressive extension of the lithosphere. *In:* Karner, G.D., Manatschal, G. & Pinheiro, L.M. (eds) *Imaging, Mapping and Modelling Continental Lithosphere Extension and Breakup*. Geological Society, London, Special Publications, **282**, 77–110.

Reston, T.J. & Phipps Morgan, J. 2004. The continental geotherm and the evolution of rifted margins. *Geology*, **32**, 133–136.

Reston, T.J., Weinrebe, W. & Grevemeyer, I. *et al.* 2002. A rifted inside corner massif on the Mid-Atlantic Ridge at 5°S. *Earth and Planetary Science Letters*, **200**, 255–269.

Reston, T.J., Ranero, C.R., Ruoff, O., Perez-Gussinye, M. & Danobeitia, J.J. 2004. Geometry of extensional faults developed at slow-spreading centres from seismic reflection data in the Central Atlantic (Canary Basin). *Geophysical Journal International*, **159**, 591–606.

Reston, T.J., Leythaeuser, T., Booth-Rea, G., Sawyer, D., Klaeschen, D. & Long, C. 2007. Movement along a low-angle normal fault. The S reflector west of Spain. *Geochemistry, Geophysics, Geosystems*, **8**, Q06002, DOI: 10.1029/2006GC001437.

Rowley, D. & Sahagian, D. 1986. Depth-dependent stretching: a different approach. *Geology*, **14**, 32–35.

Royden, L. & Keen, C.E. 1980. Rifting processes and thermal evolution of the continental margin of eastern Canada determined from subsidence curves. *Earth and Planetary Science Letters*, **51**, 343–361.

Shillington, D.J., White, N., Minshull, T.W., Edwards, G.R.H., Jones, S.M., Edwards, R.A. & Scott, C.L. 2008. Cenozoic evolution of the eastern Black Sea: A test of depth-dependent stretching models. *Earth and Planetary Science Letters*, **265**, 360–378.

Shipboard Scientific Party. 1994. Site 901. *In:* Sawyer, D.S., Whitmarsh, R.B. & Klaus, A. (eds) *Proceedings of the Ocean Drilling Program, Initial Reports*, **149**, 263–268.

Shipboard Scientific Party. 1998. Site 1065. *In:* Whitmarsh, R.B., Beslier, M.-O. & Wallace, P.J. (eds) *Proceedings of the Ocean Drilling Program, Initial Reports*, **173**, 65–104.

Sibuet, J.C. 1992. New constraints on the formation of the nonvolcanic continental Galicia–Flemish Cap conjugate margins. *Journal of the Geological Society, London*, **149**, 829–840.

Simon, N.S.C. & Podladchikov, Y.Y. 2008. The effect of mantle composition on density in the extending lithosphere. *Earth and Planetary Science Letters*, **272**, 148–157.

Thinon, I., Matias, L., Rehault, J.P., Hirn, A., Fidalgo-Gonzalez, L. & Avedik, F. 2003. Deep structure of the Armorican Basin (Bay of Biscay): a review of Norgasis seismic reflection and refraction data. *Journal of the Geological Society, London*, **160**, 99–116.

Tomasso, M., Underhill, J.R., Hodginson, R.A. & Young, M.J. 2008. Structural styles and depositional architecture in the Triassic of the Ninian and Alwyn North fields: Implications for basin development and prospectivity in the Northern North Sea. *Marine and Petroleum Geology*, **25**, 588–605.

Torsvik, T.H., Rousse, S., Labail, C. & Smethurs, M.A. 2009. A new scheme for the opening of the South Atlantic Ocean and the dissection of an Aptian salt basin. *Geophysical Journal International*, DOI: 10.1111/j.1365-246X.2009.04137.x.

Tucholke, B.E., Lin, J. & Kleinrock, M.C. 1998. Megamullions and mullion structure defining oceanic metamorphic core complexes on the mid-Atlantic ridge. *Journal of Geophysical Research*, **103**, 9857–9866.

Tucholke, B.E., Sawyer, D.S. & Sibuet, J.-C. 2007. Breakup of the Newfoundland-Iberia rift. *In:* Karner, G.D., Manatschal, G. & Pinheiro, L.M. (eds) *Imaging, Mapping and Modelling Continental Lithosphere Extension and Breakup*. Geological Society, London, Special Publications, **282**, 9–46.

Van Avendonk, H.J.A., Holbrook, W.S. & Nunes, G.T. *et al.* 2006. Seismic velocity structure of the rifted margin of the eastern Grand Banks of Newfoundland, Canada. *Journal of Geophysical Research*, **111**, B11404, DOI: 10.1029/2005JB004156.

Walsh, J.J., Watterson, J. & Yielding, G. 1991. Determination of fault populations below the limit of seismic resolution for reservoir models. *Bulletin of the American Association of Petroleum Geologists*, **75**, 688–689.

Watcharanantakul, R. & Morley, C.K. 2000. Syn-rift and post-rift modelling of the Pattani Basin, Thailand: evidence for a ramp-flat detachment. *Marine and Petroleum Geology*, **17**, 937–958.

Weinberg, R.F., Regenauer-lieb, K. & Rosenbaum, G. 2007. Mantle detachment faults and the breakup of cold continental lithosphere. *Geology*, **35**, 1035–1038.

Wernicke, B. 1985. Uniform-sense normal simple shear of the continental lithosphere. *Canadian Journal of Earth Sciences*, **22**, 331–339.

White, N. 1990. Does the uniform stretching model work in the North Sea? *In:* Blundell, D.J. & Gibbs, A.D. (eds) *Tectonic Evolution of the North Sea Rifts*. International Lithosphere Program Publication, **181**, 217–239.

White, N. & McKenzie, D.P. 1988. Formation of the "steer's head" geometry of sedimentary basins by differential stretching of the crust and mantle. *Geology*, **16**, 250–253.

White, N.J., Jackson, J.A. & McKenzie, D.P. 1986. The relationship between the geometry of normal faults and that of the sedimentary layers in their hanging-walls. *Journal of Structural Geology*, **8**, 897–909.

Whitmarsh, R.B. & Wallace, P.J. 2001. The rift-to-drift development of the west Iberia nonvolcanic continental margin: a summary and review of the contribution of Ocean Drilling Program Leg 173. *In:* Beslier, M.-O., Whitmarsh, R.B., Wallace, P.J. & Girardeau, J. (eds) *Proceedings of the Ocean Drilling Program, Scientific Results*, **173**, 1–36.

Whitmarsh, R.B., Dean, S.M., Minshull, T.A. & Tompkins, M. 2000. Tectonic implications of exposure of lower continental crust beneath the Iberia Abyssal Plain, Northeast Atlantic Ocean: Geophysical evidence. *Tectonics*, **19**, 919–942.

Wood, R. & Barton, P. 1983. Crustal thinning and subsidence in the North Sea. *Nature*, **302**, 134–136.

Zelt, C.A., Sain, K., Naumenko, J.V. & Sawyer, D.S. 2003. Assessment of crustal velocity models using seismic refraction and reflection tomography. *Geophysical Journal International*, **153**, 609–626.

Ziegler, P.A. 1983. Comment on: Crustal thinning and subsidence in the North Sea. *Nature*, **304**, 561.

Received 1 December 2008; revised typescript accepted 1 April 2009.